Helsinki University of Technology Radio Laboratory Publications
Teknillisen korkeakoulun Radiolaboratorion julkaisuja
Espoo, March 2007 REPORT S 285

ARTIFICIAL ELECTROMAGNETIC COMPOSITE STRUCTURES IN SELECTED MICROWAVE APPLICATIONS

Pekka Ikonen

Dissertation for the degree of Doctor of Science in Technology to be presented with due permission for public examination and debate in Auditorium S4 at Helsinki University of Technology (Espoo, Finland) on the 30th of March 2007 at 12 o'clock noon.

Helsinki University of Technology
Department of Electrical and Communications Engineering
Radio Laboratory

Teknillinen korkeakoulu
Sähkö- ja tietoliikennetekniikan osasto
Radiolaboratorio

Distribution:
Helsinki University of Technology
Radio Laboratory
P.O. Box 3000
FI-02015 TKK
Tel. +358-9-451 2218
Fax. +358-9-451 2152

ISBN 978-951-22-8676-8 (printed)
ISBN 978-951-22-8677-5 (pdf)
URL: http://lib.tkk.fi/Diss/2007/isbn9789512286775/

ISSN 1456-3835

Otamedia Oy
Espoo 2007

HELSINKI UNIVERSITY OF TECHNOLOGY P. O. BOX 1000, FI-02015 TKK http://www.tkk.fi	ABSTRACT OF DOCTORAL DISSERTATION

Author Pekka Ikonen

Name of the dissertation

Artificial Electromagnetic Composite Structures in Selected Microwave Applications

Date of manuscript February 19, 2007	Date of the dissertation March 30, 2007
☐ Monograph	☒ Article dissertation (summary + original articles)

Department	Electrical and Communications Engineering
Laboratory	Radio Laboratory
Field of research	Radio Engineering, Electromagnetics
Opponent(s)	Professor Nader Engeta, University of Pennsylvania
Supervisor (Instructor)	Professor Sergei Tretyakov

Abstract

Possible performance enhancement of selected microwave applications is studied using artificial electromagnetic composite structures. The following definition is adopted for artificial electromagnetic composites: If we combine two or more materials (e.g., embed metal inclusions in a dielectric matrix) to produce another material (effectively behaving as another dielectric or artificial magnetic material), this material is an artificial electromagnetic composite. By varying the inclusions and their position relative to each other it is possible to synthesize a wide variety of macroscopic material properties. Even properties that do not exist in the class of “conventional” or “natural” materials can be achieved with sophisticated design methods. This extended range of available material characteristics, or the possibility to synthesize “conventional characteristics” with more simple and cheap means, offers a new design dimension for microwave engineers.

In this thesis the focus lies in two subclasses of artificial electromagnetic composites: 1) Artificial magnetic composites; 2) Artificial dielectric composites. Most of the artificial magnetic composites considered in this work consist of periodically arranged, electrically small broken loops. The circulating currents induced to a large set of inclusions give rise to macroscopic effective permeability that exceeds unity under proper circumstances. Fundamental properties of artificial magnetic composites are studied, and the possibilities to utilize these composites as microstrip antenna substrates are explored. The obtained results indicate that artificial magnetic substrates containing only non-magnetic constituents offer no advantages in antenna miniaturization.

Artificial dielectric composites considered in this work are implemented using periodical lattices of thin conducting wires, possibly loaded with a reactive distributed impedance. The main features of so called wire medium and loaded wire medium are reviewed. Later such composites are used as artificial material for a beam shaping element in base station antenna applications. We also study plane-wave transmission through finite thickness slabs implemented using a periodical arrangement of metal wires and broken loops, and extend the vector circuit theory, previously introduced for isotropic and chiral slabs, to uniaxial and spatially dispersive magneto-dielectric slabs. Finally, the recently proposed theory of sub-wavelength field channeling is experimentally validated.

Keywords Broken loop, antenna miniaturization, wire medium, beam shaping, vector circuit, near field channeling

ISBN (printed) 978-951-22-8676-8	ISSN (printed) 1456-3835
ISBN (pdf) 978-951-22-8677-5	ISSN (pdf)
ISBN (others)	Number of pages 76 + appendix 98

Publisher Helsinki University of Technology, Radio Laboratory

Print distribution Helsinki University of Technology, Radio Laboratory

☒ The dissertation can be read at http://lib.tkk.fi/Diss/2007/isbn9789512286775

TEKNILLINEN KORKEAKOULU
PL 1000, 02015 TKK
http://www.tkk.fi

VÄITÖSKIRJAN TIIVISTELMÄ

Tekijä Pekka Ikonen

Väitöskirjan nimi

Keinotekoisten Sähkömagneettisten Komposiittimateriaalien Hyödyntäminen Eräissä Mikroaaltosovelluksissa

Käsikirjoituksen jättämispäivämäärä 19.2. 2007	Väitöstilaisuuden ajankohta 30. maaliskuuta, 2007
☐ Monografia	☒ Yhdistelmäväitöskirja (yhteenveto + erillisartikkelit)

Osasto	Sähkö- ja tietoliikennetekniikan osasto
Laboratorio	Radiolaboratorio
Tutkimusala	Radiotekniikka, sähkömagnetiikka
Vastaväittäjä(t)	Professori Nader Engheta, University of Pennsylvania
Työn valvoja (Työn ohjaaja)	Professori Sergei Tretyakov

Tiivistelmä

Tässä työssä tutkitaan eräiden mikroaaltosovellusten toiminnan parantamista hyödyntäen keinotekoisia sähkömagneettisia komposiittimateriaaleja. Työssä omaksutaan seuraava määritelmä keinotekoisille sähkömagneettisille komposiiteille: Jos yhdistetään kaksi materiaalia (esim. sekoitetaan metallikappaleita vaahtomuoviin) tarkoituksena aikaansaada uusi materiaali (joka toimii tehollisesti uudenlaisena dielektrisenä tai keinotekoisena magneettisena materiaalina), tämä uusi materiaali on keinotekoinen sähkömagneettinen komposiittimateriaali. Vaihtamalla sekoitettavia kappaleita ja niiden keskinäistä sijaintia on mahdollista syntetisoida laaja kirjo makroskooppisia materiaaliominaisuuksia. On jopa mahdollista aikaansaada materiaaliominaisuuksia, joita ei tavata nk. tavallisiksi miellettävien materiaalien joukosta. Tämä laajennettu materiaaliominaisuuksien kirjo, sekä mahdollisuus totetuttaa “tavallisia” ominaisuuksia helpommin ja halvemmin, tarjoaa tärkeän uuden sunnitteludimension mikroaaltoinsinööreille.

Työssä keskitytään kahteen keinotekoisten sähkömagneettisten komposiittimateriaalien alakategoriaan: 1) Keinotekoisiin magneettisiin komposiitteihin; 2) Keinotekoisiin dielektrisiin komposiitteihin. Useimmat tässä työssä käsiteltävät keinotekoiset magneettiset komposiitit koostuvat periodisesti asetetuista, sähköisesti pienistä metallisilmukoista. Suuressa joukossa silmukoita kiertävät virrat saavat aikaan tehollisen permeabiliteetin, joka voi olla suurempi kuin yksi. Työssä tutkitaan keinotekoisten magneettien perusominaisuuksia, sekä mahdollisuuksia hyödyntää em. komposiitteja substraatteina mikroliuska-antenneille. Väitöskirjatyön tulokset osoittavat, että pelkästään metallisilmukoista koostuvat substraatit eivät tarjoa etuja antennien miniaturisoinnissa.

Työssä käsiteltävät keinotekoiset dielektriset komposiitit toteutetaan muodostamalla periodinen hilarakenne ohuista metallilangoista. Langat voidaan myös kuormata tietyllä jakautuneella impedanssilla. Niin kutsutun lankahilarakenteen (wire medium) työn kannalta tärkeimmät ominaisuudet esitellään. Myöhemmin em. komposiitteja käytetään keinotekoisena rakennusmateriaalina tukiasema-antennien keilanmuokkauselementissä. Työssä tutkitaan myös tasoaallon etenemistä periodisesti asetettujen metallilankojen ja -silmukoiden läpi yleistämällä aikaisemmin esitetty vektoripiiriteoria uniaksiaalisille magneto-dielektrisille kerroksille. Lopuksi työssä todistetaan kokeellisesti hiljattain esitetty sähkömagneettisen lähikentän erittäin tarkkojen yksityiskohtien kanavoitumisperiaate.

Asiasanat Antennien miniaturisointi, lankahilasto, säteilykeilan muokkaus, vektoripiiri, lähikentän kanavoituminen

ISBN (painettu) 978-951-22-8676-8	ISSN (painettu) 1456-3835
ISBN (pdf) 978-951-22-8677-5	ISSN (pdf)
ISBN (muut)	Sivumäärä 76 + liitteet 98

Julkaisija Teknillinen Korkeakoulu, Radiolaboratorio

Painetun väitöskirjan jakelu Teknillinen Korkeakoulu, Radiolaboratorio

☒ Luettavissa verkossa osoitteessa http://lib.tkk.fi/Diss/isbn9789512286775

Preface

This thesis collects selected results obtained in the Radio Laboratory of Helsinki University of Technology under the supervision of Professor Sergei Tretyakov. Some of these results were outlined as an undergraduate student during 2002–2005, most of the papers presented here were finalized as a post-graduate student during 2005–2006.

Sergei, many warm thanks for the possibility to work in such a highly recognized research group all these years. Your guidance has been excellent, the way of academic thinking I tried to adopt based on your advices truly shaped the entire course of my studies. Thanks for those numerous well teaching and stimulating discussions about all kinds of aspects in radio engineering and electromagnetics.

Already as an undergraduate student I had the privilege to get to know and work with many great researchers. Unfortunately, the detailed list of all the people who have had an impact on the ideas presented here is too long to be included. Nevertheless, I wish to express my sincere gratitude collectively to all of you. My special thanks go to Dr. Stanislav Maslovski, Professor Constantin Simovski, and Dr. Pavel Belov, for helping me in the very beginning of my research work. Those early discussions and the following co-operation had a major impact on this thesis.

All my friends in and outside the Lab, many thanks for all the fun moments! Especially, I wish to thank Mr. Juha Toivanen for helping me to get a trainee position in the Radio Lab as a first year student back in 2002. Without that particular help this thesis would not have been written.

During my studies I have received financial support from Urho ja Kaisu Kiukkaan Säätiö, IEEE Antennas and Propagation Society, IEEE Microwave Theory and Techniques Society, Tekniikan Edistämissäätiö, Kaupallisten ja Teknillisten Tieteiden Edistämissäätiö, Nokia Foundation, and the Finnish Graduate School in Electronics, Telecommunication, and Automation (GETA). This support is gratefully acknowledged.

Mom, dad, Paavo, Pauliina, one of the biggest reasons for my motivation has always been the thought that some day you will share this achievement with me. Your support has been invaluable.

Thank you, my dear Liisa, for somewhere in the middle of this work reminding me about the things that really matter.

Otaniemi, February 19, 2007, P.I.

Contents

List of Publications

This thesis consists of an overview and of the following eight publications which are referred to in the text by their Roman numerals.

I S. Maslovski, **P. Ikonen**, I. Kolmakov, S. Tretyakov, and M. Kaunisto, "Artificial magnetic materials based on the new magnetic particle: Metasolenoid," in *Progress in Electromagnetics Research, PIER*, EMW Publishing, Cambridge, USA, vol. 54, pp. 61–81, 2005.

II **P. M. T. Ikonen** and S. A. Tretyakov, "Determination of generalized permeability function and field energy density in artificial magnetics using the equivalent circuit method," *IEEE Trans. Microw. Theory Tech.*, vol. 55, no. 1, pp. 92–99, 2007.

III **P. M. T. Ikonen**, S. I. Maslovski, C. R. Simovski, and S. A. Tretyakov, "On artificial magnetodielectric loading for improving the impedance bandwidth properties of microstrip antennas," *IEEE Trans. Antennas Propag.*, vol. 54, no. 6, pp. 1654–1662, 2006.

IV **P. M. T. Ikonen**, K. N. Rozanov, A. V. Osipov, P. Alitalo, and S. A. Tretyakov, "Magnetodielectric substrates in antenna miniaturization: Potential and limitations," *IEEE Trans. Antennas Propag.*, vol. 54, no 11, pp. 3391–3399, 2006.

V **P. Ikonen**, C. Simovski, and S. Tretyakov, "Compact directive antennas with a wire-medium artificial lens," *Microwave Opt. Technol. Lett.*, vol. 43, no. 6, pp. 467–469, 2004.

VI **P. Ikonen**, M. Kärkkäinen, C. Simovski, P. Belov, and S. Tretyakov, "Light-weight base station antenna with artificial wire medium lens," *IEE Proc. Microwaves, Antennas Propag.*, vol. 153, no. 2, pp. 163–170, 2006.

VII **P. Ikonen**, M. Lapine, I. Nefedov, and S. Tretyakov, "Vector circuit theory for spatially dispersive uniaxial magneto-dielectric slabs," in *Progress in Electromagnetics Research, PIER*, EMW Publishing, Cambridge, USA, vol. 63, pp. 279–294, 2006.

VIII **P. Ikonen**, P. Belov, C. Simovski, and S. Maslovski, "Experimental demonstration of sub-wavelength field channeling at microwave frequencies using a capacitively loaded wire medium," *Phys. Rev. B.*, vol. 73, 073102, 2006.

Author's contribution

In all the papers where this author is the first co-author he had the main responsibility in developing the paper. More detailed contributions are indicated below.

The author took part in the development of the analytical theory in [**I**], and in part wrote the manuscript. He also implemented and measured the prototype sample.

In [**II**] the author carried out all the derivations under the supervision of Professor Tretyakov.

The author formulated the key idea of paper [**III**], conducted all the transmission-line calculations, and implemented and measured the prototype sample.

In [**IV**] the author developed the antenna theory sections together with Professor Tretyakov.

In [**V**] the author conducted all the numerical simulations, implemented and measured the prototype antenna.

Paper [**VI**] is based on the author's Master's thesis and the author had the leading role in developing the entire paper.

In [**VII**] the author carried out all the analytical derivations and calculated the example results.

In [**VIII**] the author implemented the crystal slab and conducted the measurements. The interpretation of the results was done together with the other co-authors.

List of Abbreviations

DNG	Double negative (medium)
DSRR	Double split-ring resonator
EBG	Electromagnetic band-gap (structure)
EC	Electromagnetic crystal
GSM	Global system for mobile communications
MSRR	Modified split-ring resonator
PC	Photonic crystal
PIFA	Planar inverted F-antenna
SRR	Split-ring resonator
UMTS	Universal mobile telecommunications system

List of Symbols

I^{ind}	Amplitude of induced current
j	Imaginary unit
ω	Angular frequency
μ_0	Permeability of free space
S	Cross section area of a broken loop
H^{ext}	Amplitude of external magnetic field
Z	Impedance
$\mathbf{B}$	Magnetic flux vector
M	Magnetic dipole moment per unit volume
V_{r}	Volume filling ratio
V	(Unit) volume
μ_{eff}	Effective (relative) permeability
d	Distance between stacked broken loops in a magnetic material
	Wire diameter
C_{eff}	Effective capacitance
L_{eff}	Effective inductance
m	Magnetic dipole moment
A, B, Λ	Amplitude factor
$\omega_0, \widetilde{\omega}_0, \omega_0'$	Angular resonant frequency
$\Gamma, \Gamma_{\mathrm{d}}$	Loss factor
M	Mutual inductance
V_C, U_C, u	Amplitude of voltage
i	Amplitude of current
w	Electromagnetic field energy density
w_{e}	Electric field energy density
w_{m}	Magnetic field energy density
ϵ_0	Permittivity of free space
E	Amplitude of electric field
H	Amplitude of magnetic field
Q_{r}	Radiation quality factor
W	Stored electromagnetic energy
W_{e}	Stored electric energy
W_{m}	Stored magnetic energy
P_{r}	Radiated power
ω_{x}	Angular operating frequency of an antenna
Q_0	Unloaded quality factor
η_{r}	Radiation efficiency
G_{r}	Radiation conductance
μ_{s}	Static (relative) permeability
ω_{res}	Ferromagnetic (angular) resonant frequency
β	Empirical damping factor
M_{s}	Saturation magnetization
Y_0	Characteristic admittance

a, b	Lattice constant
λ	Wavelength
l	Insertion period for loads
q	Propagation constant in periodically loaded waveguide
	Propagation constant in wire medium
ϵ_{eff}	Effective (relative) permittivity
k_{p}	Plasma wavenumber
$\overline{\overline{I}}_t$	Tangential unit dyadic
$\mathbf{z}_0$	Unit vector along z-direction
I_{s}	Amplitude of source current
$H_0^{(2)}$	Hankel function of the second kind and zero order
n_{eff}	Effective refractive index
$\mathbf{r}$	Spatial coordinate vector
Δx	Resolution in the spatial domain
Δk	Resolution in the wave vector domain

List of Figures

1 Introduction

The ever growing complexity of communication systems added to the current application design trends sets great challenges for microwave engineers. For example, mobile phone antennas need to be downsized all the time, yet simultaneously the miniaturized antennas should retain their impedance bandwidth characteristics to eventually facilitate fast data transmission. Incorporating increasingly sophisticated performance in miniaturized and cheap communication devices clearly calls for novel design and implementation methods.

This work focuses on the utilization of artificial electromagnetic composite materials and surfaces in selected microwave applications. Here we choose to follow the definition presented in [1] for artificial electromagnetic composites: If we combine two or more materials (e.g. embed metal inclusions in a dielectric matrix) to produce another material (effectively behaving as another dielectric or artificial magnetic material), this material is an artificial electromagnetic composite. When such composites are excited by electromagnetic waves whose wavelength is large compared to the inclusion dimensions and their spacing, the waves do not "feel", or probe the fine structural details. In other words, the currents induced to the inclusions give rise to polarization effects that for the wave seem to originate from a homogeneous polarizable material. By varying the inclusions and their position relative to each other it is possible to synthesize a wide variety of macroscopic material characteristics. Actually, it is even possible to synthesize material characteristics not observed in the class of "conventional" or "natural" materials. This extended range of available material characteristics, or the possibility to synthesize "conventional characteristics" with simpler or cheaper means, is seen as a prospective and novel design tool for some microwave devices.

The rest of the thesis is organized in the following manner:

Chapter 2 outlines the results of [**I**, **II**] where we consider lattices of electrically small broken loops and study the macroscopic response of such *artificial magnetic composites*. A new magnetic particle constituting artificial magnetic composites is designed and implemented. The proposed design has several advantages compared to the previous designs. For example, the proposed stacked structure strengthens the magnetic response of the composite while it simultaneously prevents the axial current flow. We also discuss the difficulties in defining stored electromagnetic energy (equivalently electromagnetic field energy density) and dissipated power in lossy artificial magnetic composites. As a side result of this discussion, generalizations are proposed to the equivalent circuit model and macroscopic permeability function commonly used to model such composites. Further, the aforementioned generalizations lead to a new expression for the field energy density in artificial magnetic composites.

In Chapter 3 and [**III**, **IV**] we study the applicability of artificial magnetic composites as microstrip antenna substrates. Thin iron sheets, also categorized into the

class of artificial magnetic composites, are briefly introduced for the same purpose. We reduce the antenna dimensions using these exotic substrates, and study if any advantages can be gained over conventional dielectric substrates in terms of more effectively retained impedance bandwidth. The analysis reveals that, contrary to the previous opinion, arrays of broken loops do not offer any advantages over conventional dielectric substrates. It is shown that the substrates need to have static magnetic polarization and weak frequency dispersion in order to be usable. Discussion is conducted on the limitations set by practically realizable substrates on the obtainable impedance bandwidth.

In Chapter 4 and [**V**, **VI**] we study the feasibility to use a periodical lattice of metal wires as a light-weight beam shaping element in base station antenna applications. The wires in the lattice are loaded with capacitive loads in order to manipulate the dispersion properties of such *artificial dielectric composites*. It is shown that well predictable and promising radiation characteristics can be achieved with compact and cheap antenna structures. The prototype antennas are light-weight, physically simple, and the beamwidth in the horizontal plane can be switched mechanically. Compared to the solutions implemented using solid (conventional) dielectrics the advantages of the developed designs are dramatically reduced weight and cheap and simple manufacturing process.

To study plane wave transmission through finite thickness slabs implemented using periodically arranged metal wires and broken loops we extend the vector circuit theory, previously introduced for isotropic and chiral slabs, to uniaxial and spatially dispersive magneto-dielectric slabs [**VII**]. The developed method, whose background is summarized in Chapter 5, allows to study the transmission through such slabs with arbitrary plane wave incidence, and it explicitly takes into account the strong spatial dispersion in the wire medium. Example results show that the aforementioned slabs can be used as effective angular filters at microwave frequencies.

In Chapter 6 we review the key ideas behind the results of [**VIII**] where a near field channeling device operating in the microwave regime is implemented using a capacitively loaded wire medium. This channeling device is capable of transferring the near field distribution of a point source from one plane to another without losing the details of the distribution. The results presented in [**VIII**] experimentally validate the recently proposed theory of sub-wavelength field channeling [2].

Summaries of the original publications are provided at the end of the corresponding chapters. The thesis is concluded in Chapter 7.

2 Artificial magnetic composites

2.1 General

Consider an electrically small metal loop excited by a plane wave whose magnetic field penetrates the loop perpendicularly to its plane. This external magnetic field induces current to the loop and the current can be represented as the ratio between the induced electromotive force and the loop impedance:

$$I^{\mathrm{ind}} = -\frac{j\omega\mu_0 S H^{\mathrm{ext}}}{Z}, \tag{2.1}$$

where S is the cross section area of the loop, H^{ext} is the amplitude of the external magnetic field, and Z is the impedance of the loop. Let us further consider a large set of closely stacked and electrically small loops, Fig. 2.1: The separation between the loops in the stack d is small and the stacks are assumed to be infinitely long. In Fig. 2.1 the loops are broken, however, they could be closed as well. The averaged magnetic induction in the artificial material reads

$$\mathbf{B} = \mu_0 \mathbf{H}^{\mathrm{ext}} + \mathbf{M} V_{\mathrm{r}}, \quad M = \frac{\mu_0 S I^{\mathrm{ind}}}{V} \tag{2.2}$$

where $\mathbf{M}$ is the average magnetization (magnetic dipole moment per unit volume), and V_{r} is the volume filling ratio of the stacks (this is determined by the transversal separation between the stacks). In eq. (2.2) $V = S \times d$ denotes the unit cell volume (the shadowed region in the right part of Fig. 2.1). Eq. (2.2) can be rewritten in the following form:

$$\mathbf{B} = \mu_0 \mu_{\mathrm{eff}} \mathbf{H}^{\mathrm{ext}}, \quad \mu_{\mathrm{eff}} = 1 + \frac{I^{\mathrm{ind}}}{d}, \tag{2.3}$$

where we have defined the effective permeability μ_{eff} to describe the macroscopic magnetic response of the composite. We notice from (2.3) that in the quasi-static

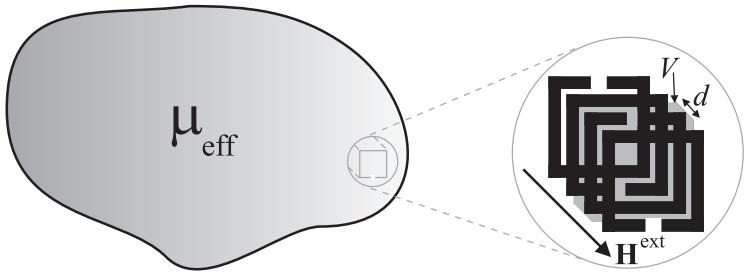

Figure 2.1: Artificial composite structure implemented using arrays of broken loops.

regime[1] the composite can be characterized macroscopically using the averaged current flowing in the loops.

Let us for the sake of clarity assume that the loops have no conductive losses (also losses due to radiation are in the following assumed to be negligible). If the loops are closed and small, their impedance can be approximated to be purely inductive [1]. In this case we notice from eqs. (2.1) and (2.3) that the effective permeability of the composite is always less than unity (we say the composite is diamagnetic). In the elementary electromagnetics this well-known phenomenon is known as the Lenz's law: The current induced to a closed loop produces a magnetic flux which weakens the change of total flux through the loop.

If we assume that the loops are broken as shown in Fig. 2.1, they can be represented as a series connection of a capacitance and inductance. At frequencies below the first resonance the impedance is dominantly capacitive, and we notice from eq. (2.1) that the current induced to the loops produces a magnetic flux which is in phase with the external flux. This gives rise to an effective permeability that exceeds unity below the loop resonance. We say the composite is paramagnetic at these frequencies.

When the broken loop is represented as a series $LC-$circuit magnetically coupled to the external field, the impedance of the loop reads

$$Z = \frac{1}{j\omega C_{\text{eff}}} + j\omega L_{\text{eff}}, \tag{2.4}$$

where $C_{\text{eff}}, L_{\text{eff}}$ are the effective circuit parameters of the loop. In this case the amplitude of the magnetic dipole moment can be derived in the following form

$$m = \mu_0 S I^{\text{ind}} = \frac{\omega^2 \mu_0^2 S^2 C_{\text{eff}} H^{\text{ext}}}{1 - \omega^2 L_{\text{eff}} C_{\text{eff}}}. \tag{2.5}$$

Eq. (2.5) tells us that at low frequencies the dipole moment is proportional to the effective capacitance. Thus, in order to strengthen the magnetic response of the composite we should increase C_{eff} as much as possible.

As a summary we conclude that artificial magnetism arises from circular currents induced in electrically small inclusions. The current in the loop must obey a resonant dependence in order for the composite to behave as an effective paramagnetic material. One of the important design goals of artificial magnetics is the increase of the effective capacitance as much as possible: This will strengthen the magnetic response and allow the realization of higher effective permeability values.

[1] At frequencies when the loop dimensions and their spacing are small compared to the wavelength.

Additional comments

1) It is worth to note that the analysis presented above is rather simplified as the idea is to give a simple physical understanding behind broken-loop composites. A more detailed analysis of the input impedance of electrically small loop antennas reveals that the impedance is not purely inductive [3]. Detailed polarization studies of broken-loop particles (see e.g. [1, Ch. 5], [4]) indicate that due to the non-uniform current distribution in the loaded loop the loop should be interpreted as a bi-anisotropic particle. Thus, electric field will also induce magnetic polarization, and magnetic field will induce electric polarization. However, by properly choosing the geometrical structure of the inclusions the bi-anisotropic effects can be minimized. For example, by stacking two loops together the whole structure can in the quasi-static regime be represented as one "effectively" loaded loop having uniform current distribution [4], [**I**].

2) In a finite sample of a medium made of stacked loops the neighboring stacks interact because the flux escaping from the end of one stack penetrates into another one. Interaction between finite size Swiss rolls (a magnetic particle introduced later in a more detail) was mentioned based on experimental results in [5], and it was concluded that at frequencies below the resonance (in the quasi-static regime) the role of interaction is much less significant than at frequencies just above the resonance. Because in the above analysis such interactions are not taken into account, the analysis is applicable either when the stacks are in such condition that they can be considered as effectively infinite, or when the operational frequency is well below the particle resonance. In the latter case magnetization is distributed rather uniformly even in finite length stacks.

2.2 Equivalent circuit model and macroscopic permeability function

If we build an artificial magnetic composite by embedding broken loops in a lossless matrix like shown in Fig. 2.1, the effective permeability can be cast in the following form

$$\mu_{\text{eff}} = 1 + \frac{\frac{\mu_0 S}{Ld}\omega^2}{\frac{1}{LC} - \omega^2 + j\omega\frac{R}{L}} = 1 + \frac{A\omega^2}{\omega_0^2 - \omega^2 + j\omega\Gamma}, \tag{2.6}$$

where A represents the amplitude factor, ω_0 the composite resonant frequency, and Γ the loss factor. Expression (2.6) looks similar to the classical Lorentz model (see e.g. [6]) with the exception that we have the squared angular frequency in the nominator instead of the squared angular plasma frequency. Eq. (2.6) is obviously applicable only in the quasi-static regime since in the limit $\omega \to \infty$ the permeability does not tend to μ_0. At extremely high frequencies materials cannot be polarized due to inertia of electrons, thus, a physically sound high frequency limit is μ_0 [7]. However, at very high frequencies our main assumption that the loops are small compared to the wavelength is violated, and it is not meaningful to try to introduce effective material parameters. The other relevant restriction on the permeability

function is the inequality [7]

$$\frac{\partial(\omega\mu_{\text{eff}})}{\partial\omega} > 1, \tag{2.7}$$

valid in the frequency regions with negligible losses. Physically the above restriction means that the stored energy density in a passive linear lossless medium must always be larger than the energy density of the same field in vacuum. Macroscopic model (2.6) violates restriction (2.7) at high frequencies, which is another manifestation of the quasi-static nature of the model.

Consider next the unit cell volume containing one loop and shown shadowed in the right part of Fig. 2.1 (we call this the unit cell). Moreover, assume that the unit cell is positioned in the magnetic field of a tightly wound long solenoid, i.e. the unit cell is positioned in a uniform magnetic field as depicted in the circuit level in Fig. 2.2a. If we assume that the host matrix for the loops (in practice the dielectric laminate on which the loops are printed) has no losses, the equivalent circuit of the solenoid with the unit cell is that shown in Fig. 2.2b. The circuit model is physically sound since the modeled structure is a small loop (represented as a series resonant contour) magnetically coupled to the external magnetic field. Moreover, the impedance of the solenoid (calculated based on the circuit in Fig. 2.2b) reads

$$Z(\omega) = j\omega L_0 + \frac{j\frac{M^2}{L}\omega^3}{\frac{1}{LC} - \omega^2 + j\omega\frac{R}{L}} = j\omega L_0\left(1 + \frac{\frac{M^2}{LL_0}\omega^2}{\frac{1}{LC} - \omega^2 + j\omega\frac{R}{L}}\right), \tag{2.8}$$

where the bracketed expression denotes the effective permeability, and it has the same form as (2.6). Fig. 2.3 shows a typical frequency dependence of the effective permeability of artificial magnetic composites. We notice that due to the resonating inclusions the composite is highly dispersive and shows strong losses at frequencies where the magnetic response is strongest.

It is worth to note, however, that in reality the host matrix for the loops is always lossy. The equivalent circuit in this case is that shown in Fig. 2.2c [**II**]. When we derive the impedance of the solenoid based on the aforementioned circuit we notice that in this case (2.6) is an insufficient macroscopic model for the artificial material.

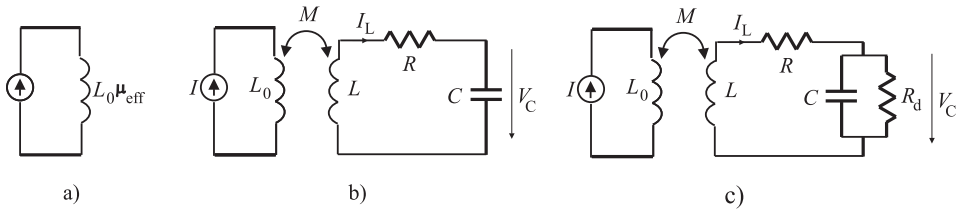

Figure 2.2: a) Broken loop in the magnetic field of a long solenoid. b) Equivalent circuit when the host matrix is lossless. c) Equivalent circuit when the host matrix has losses. M denotes mutual inductance.

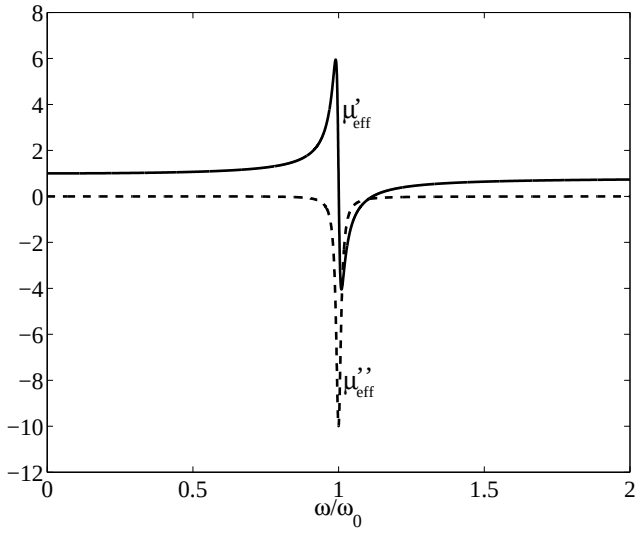

Figure 2.3: Real (μ'_{eff}) and imaginary (μ''_{eff}) parts of the effective permeability of a certain artificial magnetic composite. Amplitude factor $A = 0.2$, loss factor $\Gamma = \omega_0/50$ in (2.6).

Using the reasoning presented above we can derive the following permeability model for the composite [**II**]:

$$\mu_{\text{eff}} = 1 + \frac{A\omega^2 - j\omega B}{\widetilde{\omega}_0^2 - \omega^2 + j\omega(\Gamma + \Gamma_{\text{d}})}, \tag{2.9}$$

where A, B are the amplitude factors, $\Gamma, \Gamma_{\text{d}}$ are the loss factors due to finite conductivity and substrate losses, respectively, and $\widetilde{\omega}_0$ is the resonant frequency of the composite (which is affected by the losses).

2.3 On stored energy and dissipated power

At this stage we know the microstructure (equivalent circuit) of artificial magnetic composites, and the corresponding macroscopic permeability function. We would still like to know what is the energy stored and power dissipated in the composite with a given excitation field. Moreover, we would like to be able to define stored electromagnetic energy (field energy density) also near the resonance of the composite where losses clearly are not negligible anymore, Fig. 2.3.

It is well explained in reference books (e.g. [7, 8]) that for the definition of stored electromagnetic energy (equivalently field energy density) in a material having non-negligible losses one always needs to know the material microstructure. First of all, the reactive energy stored in any material sample is a quantity that can be

measured. When the material is *lossless*, no information is needed about the material microstructure for this measurement. Indeed, we can measure the total power flux through the surface of a sample volume[2] and, since there is no power loss inside, we can use the Poynting's theorem to determine the change in the stored energy. This is the reason why the field energy density in a dispersive medium with negligible losses can be expressed through the frequency derivative of macroscopic material parameters (e.g. [7]):

$$w = w_{\mathrm{e}} + w_{\mathrm{m}} = \frac{\epsilon_0}{2}\frac{\partial(\omega\epsilon_{\mathrm{eff}})}{\partial\omega}|E|^2 + \frac{\mu_0}{2}\frac{\partial(\omega\mu_{\mathrm{eff}})}{\partial\omega}|H|^2. \tag{2.10}$$

Above E, H are the peak amplitudes of the electric and magnetic field, respectively. In the circuit theory, the aforementioned conclusion is true for circuits that contain only reactive elements: It is possible to find the stored reactive energy in the whole circuit knowing only the input impedance of a two-port [9].

Simple reasoning reveals, that in the presence of non-negligible material losses the above described "black box" representation and direct measurement are not applicable: Without knowing the material microstructure or the circuit topology we do not know which portion of the input power is dissipated and which is stored in the reactive elements. Thus, the energy stored in lossy media cannot be *uniquely* defined by only utilizing the knowledge about the macroscopic behavior of the media [7, 8]. Thus, (2.10) is valid only at frequencies where absorption due to losses can be neglected.

In the recent literature there have been attempts to derive the field energy density in a lossy artificial magnetic material using the so called electrodynamic method [10,11]: One first writes down the "equation of motion" for magnetization density in the material using the macroscopic material model (2.6). We have to bear in mind, however, that this equation is *macroscopic* equation of motion, containing the same physical information as the macroscopic permeability function. Further, complex Poynting theorem is used to identify the mathematical form of the general macroscopic energy density expressions. Having the form of these expressions in mind one searches for similar expressions using the equation of motion and defines them as energy densities. The problem of such method is that it only utilizes the knowledge about the macroscopic behavior of the material, which, as explained above, in not enough. However, as soon as we know the microstructure of the material and physically sound equivalent circuit model, the stored energy (field energy density) and the dissipated power can be uniquely calculated using the classical circuit theory [8, 12], [**II**].

2.4 Review of related results found in the literature

2.4.1 Magnetic particles

Fig. 2.4 shows schematically some of the inclusions (particles) introduced in the literature in connection with artificial magnetic materials. The broken loop (Fig. 2.4a) was introduced as an artificial magnetic particle already in the 1950's [13]. Authors of [14] considered a cylinder having a gap on its surface parallel to the cylinder axis, and called such a structure split-ring resonator (SRR). In 1980's and 1990's loop shaped particles (often combined with other geometries) were studied a lot in connection with the development of chiral media for microwave applications [15]. Artificial magnetism exists also in bi-anisotropic composites where the inclusions have spiral shapes [16]. In the beginning of 1990's the magnetic response of lattices of closed loops was studied in [17], and in [18, 19] the authors considered lattices of broken loops and demonstrated the paramagnetic response of such lattices.

In 1999 Pendry and co-authors introduced the "Swiss roll" (a metal sheet wound on a cylinder form, Fig. 2.4b) and the SRR having the geometry shown in Fig. 2.4c[3] [20]. The resonant properties of individual and coupled DSRRs have been studied e.g. in [21, 22], and a detailed study of the polarization effects of DSRRs can be

[2]In practise the measurement can be done, for example, by positioning a material sample inside a parallel plate waveguide and measuring the S_{11} and S_{21} parameters.

[3]To make a distinction between the broken loop (also commonly referred to as SRR) and the particle shown in Fig. 2.4c, we call the latter "double split-ring resonator" (DSRR).

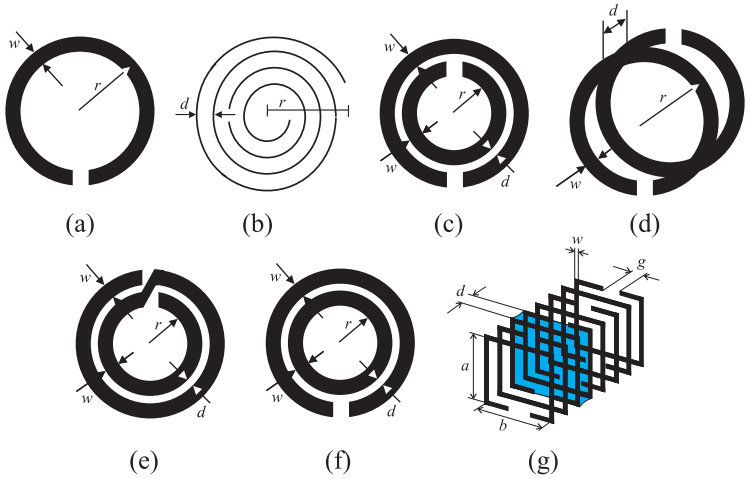

Figure 2.4: Different inclusions used to implement artificial magnetic composites: a) broken loop, b) cross section of a Swiss roll, c) double split-ring resonator (DSRR), d) modified split-ring resonator (MSRR), e) two turn spiral resonator, f) singly split double ring, g) metasolenoid.

found in [23]. Marqués *et al.* studied the bi-anisotropic effects of a material formed by DSRRs [4], and introduced the modified split-ring resonator (MSRR) as a new inclusion to avoid bianisotropic effects, Fig. 2.4d. Authors of [24] later developed a quasi-analytical model to calculate the polarizabilities of MSRRs. Lagarkov and co-authors studied the magnetic properties of composites consisting of compensated wire helixes [25], and authors of [26] proposed to use a planar spiral (Fig. 2.4e) to reduce the unit cell size and weaken magnetoelectric coupling. Shamonin and co-authors modified in [27] the DSRR by enclosing the inner ring, and studied the resonant properties of this kind of a "singly split double ring", Fig. 2.4f. The particle proposed in this thesis, *metasolenoid* [**I**], is shown in Fig. 2.4g. Authors of [28] later extended the analysis of [**I**] and studied the higher order resonant modes of the metasolenoid.

2.4.2 Electromagnetic field energy density

The procedure for defining electromagnetic field energy density in a continuous dispersive medium with negligible losses has been discussed in detail e.g. in [7–9, 29]. The definition of the field energy density in the presence of non-negligible losses is not so straightforward, as was explained earlier (refs. [7, 8] provide an extensive related discussion). In the 1970's Askne and Lind made an attempt for this definition using the effective material parameters [30]. In [31] Loudon derived the energy density expression for an absorbing Lorentz type dielectric starting from the macroscopic equation of motion for the electric charge density. Loudon's approach has recently been reviewed/extended in [10, 11, 32].[4] Tretyakov used in [12] another method: Starting from the material microstructure, an equivalent circuit representation was derived for the unit cell constituting specific artificial dielectric and magnetic media. Lattices of thin wires and arrays of split-ring resonators were considered in [12]. The stored reactive energy and field energy density were calculated using the classical circuit theory. In connection with antenna theory, Yaghjian postulated in [34] that field energy density in highly dispersive and lossy materials could be calculated by substituting the absolute values of complex material parameters in the classical expression (2.10).

2.5 Contributions of this thesis (summary of related publications)

1. In [**I**] we design and experimentally characterize a new artificial magnetic particle, *metasolenoid*, Fig. 2.4g. Compared to the particles introduced earlier the proposed particle has several practical advantages: The metasolenoid consists of closely stacked loops, thus, the dominant capacitance arises from the capacitance between the stacked loops. The structure geometry therefore allows the realization of high effective capacitance values leading to a strong magnetic response, and prevents the magnetic flux lines from escaping outside

[4] While this manuscript was in preparation a recent article [33] was published. The analysis of [33] is also essentially based on the macroscopic equations of motion.

the metasolenoid. As a result of the strengthened magnetic response the metasolenoid composite shows high values for the effective permeability over a noticeably wider range of frequencies *far away from the particle resonance* as compared to earlier composites.

The metasolenoid can also be considered and realized as a Swiss roll (Fig. 2.4b) cut into many individual parallel rolls. A clear advantage compared to the Swiss roll is the fact that the metasolenoid prevents axial current flow. This can be important e.g. if an array of metasolenoids is utilized in antenna geometries where the electric field has a component parallel to the particle axis. In addition to this, according to the author's knowledge, all the present Swiss roll realizations have been targeted only to radio frequencies whereas the metasolenoid can easily be designed and implemented for GHz frequencies.

2. In [**II**] we conduct detailed discussion on two different methods used to define field energy density in lossy artificial magnetic materials. The discussion reveals that the stored energy (equivalently field energy density) can be uniquely defined only at the microscopic level of the material.

   A generalization is proposed for the equivalent circuit model of artificial magnetic materials introduced in [12]. The proposed circuit model takes into account losses in the host matrix (substrate on top of which the loops are printed). It is shown that the generalization forces a modification to the commonly accepted permeability function used to macroscopically model these structures. The proposed equivalent circuit model and permeability function are experimentally validated. Further, we derive a generalized expression for the magnetic field energy density in artificial magnetic materials.

3 Artificial magnetic composites as microstrip antenna substrates

3.1 Introduction

The traffic load in the wireless networks is expected to grow in the near future [35]. At the same time the trend in the communications industry favors smaller size hand-held devices. This kind of an environment is very challenging for antenna designers because small devices mean small antennas. The situation is especially demanding as the smaller size antennas should not lose their capability to fulfill the ever tightening system requirements. For example, the downsized antennas should retain their impedance bandwidth characteristics as effectively as possible.

Microstrip antennas (e.g. the planar inverted F-antennas, PIFAs) are one of the most commonly used antenna types in hand-held devices, such as mobile phones. The number of articles analyzing different microstrip antenna configurations for use in communications devices is big and rapidly growing (an interested reader might want to start e.g. from [36–38]). Also several miniaturization techniques have been proposed for microstrip antennas, however, most of them can be categorized into one of the two "main" miniaturization methods: 1) Current path manipulation on the antenna element; 2) Material loading. Here we concentrate on the second method but keep in mind that a combination of both methods might in some cases lead to the optimal performance.

In this chapter we analyze a $\lambda/2$-patch antenna lying on top of a substrate and backed by a non-resonant ground plane. Though the antenna geometry is not directly applicable e.g. for use in mobile phones (due to the large ground plane), this geometry introduces a very fundamental problem: If we are free to choose the substrate material parameters, what are the parameters that will allow us to achieve the widest impedance bandwidth after size reduction? And as importantly, are we able to synthesize such material parameters? Here we consider different substrates which all offer the same size reduction, i.e. the miniaturized antennas have the same volume and the resonant frequency. Moreover, it is assumed that the substrates do not alter the current and voltage distributions on the antenna. Our figure of merit in this work will be the radiation quality factor

$$Q_\mathrm{r} = \left.\frac{\omega W}{P_\mathrm{r}}\right|_{\omega=\omega_\mathrm{x}} = \frac{Q_0}{\eta_\mathrm{r}}, \tag{3.1}$$

where ω_x is the operational angular frequency of the antenna, W denotes the amount of stored energy in the volume defined by the near fields of the antenna, P_r is the power radiated by the antenna during one cycle, Q_0 is the unloaded quality factor, and η_r is the radiation efficiency. The impedance bandwidth is inversely proportional to Q_0, so our goal clearly is to minimize Q_r. However, losses in the material must be low, as high losses strongly degrade η_r and Q_r increases correspondingly.

3.2 Desired substrate parameters

Let us consider a resonant $\lambda/2$-patch antenna operating at the fundamental angular frequency ω_{x}. Moreover, assume at this stage the antenna to be filled with a certain hypothetical dispersion-free and lossless material characterized by μ, ϵ, Fig. 3.1a. At the resonance the amplitude of the current oscillating in the antenna element $|I_{\mathrm{L}}|$ can be very strong (compared to the input current i). In the antenna structure presented in Fig. 3.1a the strong current flowing in the antenna element (and in the ground plane) creates a flux which only contributes to the stored energy, since radiation takes place at the edges of the patch. Moreover, if one leaves the ends of the patch free from the filling (as is done in Fig. 3.1a), the filling has only a very small effect on the radiation conductance. So intuitively one should try to decrease the amplitude of the oscillating current as much as possible.

The impedance behavior of the antenna can be approximated with the behavior of a parallel resonant circuit in the vicinity of ω_{x}, Fig. 3.1b. If we load the antenna with a dielectric material, the increase in C^{a} will lower the impedance of the capacitor, moreover at the same time we must decrease L^{a} (to keep ω_{x} fixed), which further leads to a decreased impedance level. Thus, it will be easy for the oscillation to build up in the circuit. The same observation will be seen by considering the stored energy in the circuit at the resonance

$$W = \ W_{\mathrm{e}} + W_{\mathrm{m}} = \frac{L^{\mathrm{a}}}{2}|I_L|^2 + \frac{C^{\mathrm{a}}}{2}|U_C|^2 = \frac{|U_C|^2}{2}\left(\frac{1}{\omega^2 L^{\mathrm{a}}} + C^{\mathrm{a}}\right), \tag{3.2}$$

where $|U_C|$ is the amplitude of the voltage over the capacitor. Usually a patch antenna is fed with a fixed voltage source, thus, $|U_C|$ is fixed. We see from (3.2) that increase in C^{a} leads to strongly increased stored energy, since we must at the same time decrease the value of L^{a} to keep the resonant frequency fixed. On the other hand, by increasing L^{a} we can reduce C^{a} and both factors decrease the stored

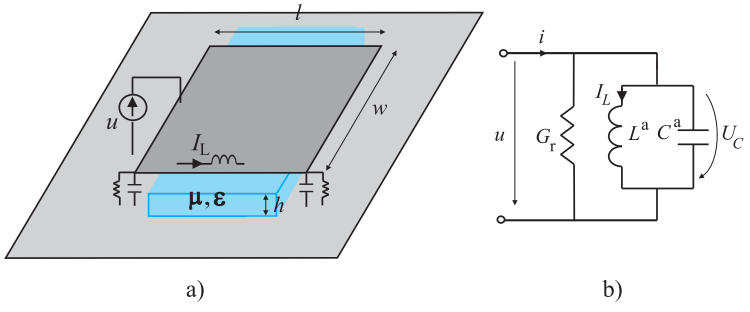

Figure 3.1: a) Schematic illustration of a patch antenna fed with a voltage source. The antenna is loaded with a certain low-loss material. b) Equivalent circuit representation in the vicinity of the fundamental resonant frequency.

energy (compared to the previous case), and further, the quality factor.

The simple analysis presented above gives us a hint that in order to retain the impedance bandwidth characteristics most effectively we should use *a magnetic substrate* with high effective permeability and low permittivity. This observation is actually well known in the literature.

It is known that when the antenna dimensions are reduced using high permittivity dielectrics, the impedance bandwidth suffers significantly [39–45]. High permittivity dielectrics are also known to lead to the excitation of surface waves and difficulties in the impedance matching of the antenna. It is explicitly mentioned already in the work of Jackson and Alexopoulos [46] that the impedance bandwidth of a patch antenna decreases inversely with increasing the substrate permittivity ϵ_{eff} (for a fixed substrate thickness), while the substrate permeability μ_{eff} has only a little effect (authors of [46] considered lossless and dispersion-free materials). The aforementioned observation was later brought into the attention of a more wide audience by Hansen and Burke [47], who demonstrated using a transmission-line analysis that when the material parameters of the antenna substrate are dispersion-free and lossless, and $\mu_{\text{eff}} \gg \epsilon_{\text{eff}}$, $\mu_{\text{eff}} \gg 1$, the impedance bandwidth of a $\lambda/2$-patch antenna is retained after miniaturization [47]. Edvardsson [48] derived an expression for the radiation quality factor Q_{r} of a material-loaded PIFA, and concluded that a high-permeability substrate allows size reduction without increasing Q_{r}.

3.3 Practically realizable magnetic substrates

Dispersion-free high-permeability materials are of course hypothetical, as is clear from causality. Moreover, it seems unlikely to achieve condition $\mu_{\text{eff}} \gg \epsilon_{\text{eff}}$, $\mu_{\text{eff}} \gg 1$ at microwave frequencies, especially with low associated losses. From the literature we know two options how to implement magnetic substrates for microstrip antennas. We can either use

1. composites consisting of arrays of electrically small broken loops, or
2. composites containing ferromagnetic (ferrimagnetic) inclusions.

3.3.1 Broken-loop composites

Broken-loop composites were analyzed in the previous section and we used (2.9) to describe their macroscopic magnetic behavior. As we see from Fig. 2.3, to achieve microwave permeability values exceeding unity we must operate close to the resonance of the composite. This means that the substrate implemented using broken loops is highly dispersive, and the analysis based on hypothetical dispersion-free high-permeability substrates will not be sufficient. In fact, in this case it is more

appropriate to speak about a system of two coupled resonators, rather than a resonator filled with a static paramagnetic load. Indeed, the current flowing in the antenna element (and in the ground plane) creates a magnetic flux which excites the loops (the magnetic field vector should be oriented like shown in Fig. 2.1 with respect to the loops). Thus, the configuration is very similar to the situation of Fig. 2.2a, except that the non-uniform flux and the finite composite size weaken the magnetic response of the composite. The equivalent circuit of the loaded antenna in the vicinity of ω_{x} is obviously that shown in Fig. 3.2.

Typically in the quasi-static regime the substrate has only a weak contribution to radiation, thus, the radiation quality factor can be calculated directly based on the presented circuit model:

$$Q_{\mathrm{r}} = \frac{\omega(W^{\mathrm{p}} + W^{\mathrm{s}})}{P_{\mathrm{r}}}, \tag{3.3}$$

where W^{p} is the energy stored in the parallel circuit representing the antenna (patch) element, W^{s} is the energy stored in the substrate, and the radiated power reads

$$P_{\mathrm{r}} = G_{\mathrm{r}}|u|^2, \tag{3.4}$$

where G_{r} is the radiation conductance. Using the introduced circuit model we can derive the following expression for the radiation quality factor:

$$Q_{\mathrm{r}} = \frac{\omega}{2G_{\mathrm{r}}}\left(C^{\mathrm{a}} + \frac{1}{\omega^2 L^{\mathrm{a}}} + \frac{\frac{M^2}{(L^{\mathrm{a}})^2 L}\left(\frac{1}{LC} + \omega^2 + \frac{1}{C^2 R_{\mathrm{d}}^2}\right)}{[(1+\frac{R}{R_{\mathrm{d}}})\frac{1}{LC} - \omega^2]^2 + \omega^2(\frac{R}{L} + \frac{1}{CR_{\mathrm{d}}})^2}\right)\Bigg|_{\omega=\omega_{\mathrm{x}}}. \tag{3.5}$$

Expression (3.5) is general, however, it does not readily tell how the radiation quality factor depends, for example, on the substrate height or the width of the antenna element. To utilize (3.5) one has to 1) estimate the values for the effective circuit parameters and 2) solve the angular resonant frequency from the condition $\mathrm{Im}\{Y_{\mathrm{in}}\} = 0$, where Y_{in} is the input admittance of the loaded antenna. Another way to find the stored energy, and further Q_{r}, is to integrate the expression for the electromagnetic field energy density over the volume of the antenna. We will discuss

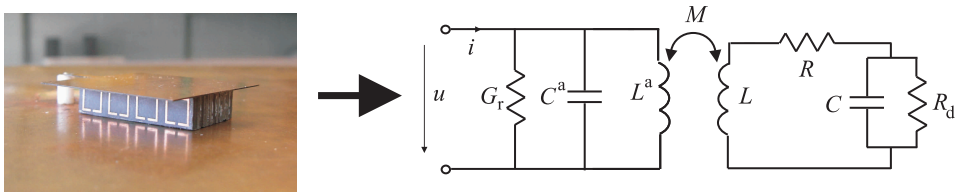

Figure 3.2: Left: Prototype of a microstrip antenna loaded with an artificial magneto-dielectric substrate [**III**]. Right: Equivalent circuit model in the vicinity of the fundamental operational frequency of the antenna.

this later.

3.3.2 Composites containing ferromagnetic inclusions

In this work we mean by ferromagnetic inclusions thin iron sheets. Blocks of ferrite materials (e.g. the Z-type hexaferrite) are typically categorized into the class of ferrimagnetic inclusions, however, their macroscopic magnetic behavior resembles that of ferromagnetics. The main importance for the present work is the fact that composites containing the aforementioned inclusions show static magnetic polarization (static effective permeability μ_s exceeds unity). Thus, they are fundamentally different from the substrates implemented using arrays of broken loops where non-magnetic constituents are used to enhance magnetic phenomenon. Below we focus only on composites containing ferromagnetic inclusions.

When modeling composites containing ferromagnetic inclusions the Lorentz model is commonly used for the complex permeability [49, 50]:

$$\mu_\mathrm{eff} = 1 + \frac{(\mu_\mathrm{s}-1)\omega_\mathrm{res}^2}{\omega_\mathrm{res}^2 - \omega^2 + j\omega\beta\omega_\mathrm{res}} = \mu_\mathrm{s} + \frac{(\mu_\mathrm{s}-1)\omega^2 - j\omega(\mu_\mathrm{s}-1)\beta\omega_\mathrm{res}}{\omega_\mathrm{res}^2 - \omega^2 + j\omega\beta\omega_\mathrm{res}}, \tag{3.6}$$

where μ_s is the static permeability, ω_res is the ferromagnetic (angular) resonant frequency, and β is an empirical damping factor. The complex permeability is close to the static permeability μ_s at frequencies up to the ferromagnetic resonant frequency ω_res, which can be considered as the permeability cutoff frequency. The microwave permeability is large when both μ_s and ω_res are high, however, these values are related tightly to each other: Higher μ_s leads to lower ω_res, and vice versa. In case of thin ferromagnetic films with in-plane magnetic anisotropy the relation between the static permeability and resonant frequency has the form [51, 52]

$$(\mu_\mathrm{s}-1)\cdot {\omega_\mathrm{res}}^2 = c(\gamma 4\pi M_\mathrm{s})^2, \tag{3.7}$$

where $4\pi M_\mathrm{s}$ is the saturation magnetization and $\gamma \approx 3$ GHz/kOe. With thin ferromagnetic films $c \approx 4\pi^2$ and μ_s is the largest component of permeability.

Fig. 3.3 shows a typical frequency dependency for the effective permeability of a certain composite consisting of thin iron sheets. We notice that the dispersion in the composite is weaker than in the array of broken loops. Based on Fig. 3.3 we conclude that with the above introduced composites it is possible to achieve weakly dispersive microwave permeability values that exceed unity. However, losses in the composite strongly increase as the frequency increases.

3.4 Relative radiation quality factor

At this point we know that dispersion-free high-permeability (magnetic) substrates are desirable in antenna miniaturization in the view of retained impedance band-

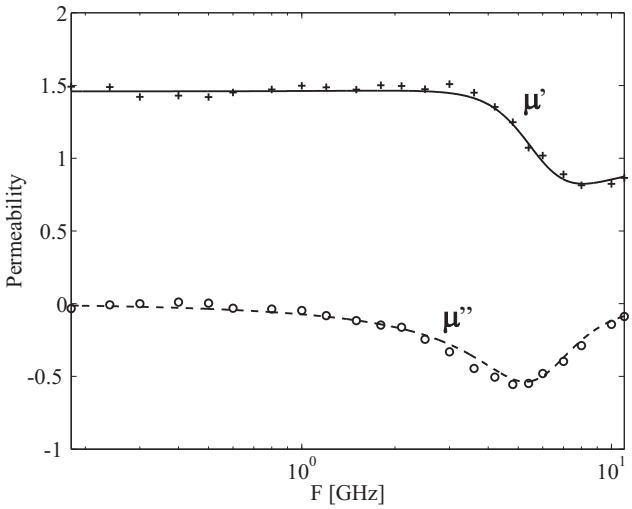

Figure 3.3: Effective permeability of a composite consisting of thin iron sheets [**IV**]. Lines fit the experimental data (crosses and circles) to the permeability model (3.6).

width. We are also well aware of the fact that due to causality restrictions the aforementioned substrates are hypothetical. Two possibilities to implement magnetic substrates have been proposed above, and we know how to model the proposed substrates macroscopically. Here our aim is to derive an expression that allows us to see if any of the proposed substrates offers advantages over conventional high-permittivity dielectrics in antenna miniaturization.

To ease the comparison between Q_r obtained using different substrates we assume in the following that losses in the substrate are small at the operational frequency of the antenna ω_x. This assumption is justified by the fact that typically the resonant frequency of the loaded antenna is well below the resonance of the magnetic substrate $\omega_\mathrm{x} \ll \omega_0, \omega_\mathrm{x} \ll \omega_\mathrm{res}$.[5] Note that at this point we consider a general case of frequency dispersion, the low-loss assumption is the only assumption that we make concerning the dispersion law in the material.[6] We consider the resonant $\lambda/2$-patch antenna shown in Fig. 3.1a and calculate the energy stored in the antenna volume by integrating (2.10) over the antenna volume. The radiated power is calculated

[5]The electric resonance of arrays of small broken loops lies at a very high frequency compared to the magnetic resonance. Thus, it is in the following assumed that the permittivity of such composites is dispersion-free. With composites containing thin iron sheets the permittivity can also be assumed to be dispersion-free over a wide frequency range [50].

[6]However, since operation of the considered antennas in based on resonant antenna element length, both permittivity and permeability of the substrate must be simultaneously either positive or negative.

using (3.4), and the quality factor takes the following form [**III**]:

$$Q_{\mathrm{r}} = \frac{\pi Y_0}{8G_{\mathrm{r}}}\left(\frac{1}{\mu_{\mathrm{eff}}}\frac{\partial(\omega\mu_{\mathrm{eff}})}{\partial\omega}\bigg|_{\omega=\omega_{\mathrm{x}}} + \frac{1}{\epsilon_{\mathrm{eff}}}\frac{\partial(\omega\epsilon_{\mathrm{eff}})}{\partial\omega}\bigg|_{\omega=\omega_{\mathrm{x}}}\right), \tag{3.8}$$

where Y_0 is the characteristic admittance of the patch segment (wide microstrip) [42], and $\mu_{\mathrm{eff}}, \epsilon_{\mathrm{eff}}$ are the effective substrate material parameters.

When studying antenna miniaturization using novel antenna substrates, conventional dielectric substrates should be used as a reference substrate. Usually with high accuracy the permittivity of the substrate can be regarded dispersion-free over a wide frequency range. Let us in the reference case fill the volume under the antenna element with a dielectric substrate offering the same size reduction [$\epsilon_{\mathrm{eff}}^{\mathrm{ref}} = \mu_{\mathrm{eff}}(\omega_{\mathrm{x}})\epsilon_{\mathrm{eff}}(\omega_{\mathrm{x}})$]. The ratio between the radiation quality factors becomes [**III**, **IV**]

$$Q_{\mathrm{r}}^{\mathrm{rel}} = \frac{Q_{\mathrm{r}}}{Q_{\mathrm{r}}^{\mathrm{ref}}} = \frac{1}{2\mu_{\mathrm{eff}}}\left(\frac{1}{\mu_{\mathrm{eff}}}\frac{\partial(\omega\mu_{\mathrm{eff}})}{\partial\omega}\bigg|_{\omega=\omega_{\mathrm{x}}} + \frac{1}{\epsilon_{\mathrm{eff}}}\frac{\partial(\omega\epsilon_{\mathrm{eff}})}{\partial\omega}\bigg|_{\omega=\omega_{\mathrm{x}}}\right). \tag{3.9}$$

(Another technique to derive eq. (3.9) starting from the input impedance of patch antennas in presented in [53].) Eq. (3.9) is the key formula allowing a proper comparison between the impedance bandwidth characteristics of rectangular[7] patch antennas loaded with conventional dielectric substrates and novel antenna substrates. It can be used when the following criteria are met:

1. The antennas operate in the fundamental parallel resonant mode.
2. Both substrates contain only passive inclusions and have small losses.
3. The reference substrate does not possess any magnetic response and the permittivity can be considered dispersion-free.
4. Both substrates fill the volume under the patch element uniformly (the substrates do not reshape the induced resonant standing-wave pattern).
5. The substrates do not couple to the radiating modes of the antenna (the radiation conductance is the same for both antennas).

3.4.1 Example results

We can see from eqs. (2.9) and (3.6) that both reduce to a similar looking expression when losses in the material are small:

$$\mu_{\mathrm{eff}} = \mu_{\mathrm{s}} + \frac{\Lambda\omega^2}{\omega_0'^2 - \omega^2}, \tag{3.10}$$

[7]The aforementioned steps of derivation can be repeated for different antenna geometries.

where Λ denotes the amplitude factor and ω_0' the angular resonant frequency of the composite. With broken loop composites $\mu_s = 1$, with composites containing ferromagnetic inclusions $\mu_s > 1$. In the following we fix ω_0' and plot Q_r^{rel} with different amplitude factors. We consider separately broken-loop composites and composites containing thin iron sheets.

1) Broken-loop composites [$\mu_s = 1$ in (3.10)].

The relative radiation quality factor is depicted in Fig. 3.4a, and we make a very important observation: Q_r^{rel} exceeds unity over the entire feasible[8] frequency range, i.e. the impedance bandwidth obtained using broken-loop composites is *always more narrow* than the bandwidth obtained using conventional dielectrics. The positive effect of enhanced microwave permeability is outweighed by the very strong associated dispersion.

The result shown in Fig. 3.4a is physically rather intuitive: The substrate consists of small resonating inclusions, thus, work has to be done to polarize the inclusions for their microwave performance. Moreover, since the inclusions do not contribute to radiation, the power will be stored in the reactive near fields. According to the author's understanding the only way to gain advantages with a resonant substrate is to couple it to the radiating modes of the antenna. This observation was already made in [54] for material covered line sources. However, if the inclusions are coupled to radiation we are not actually anymore speaking about material loading, rather

[8]Eq. (3.9) is not valid in the frequency range where $\mu_{eff} < 0, \epsilon_{eff} > 0$ since at these frequencies no resonance due to electrical length can be assigned to the antenna. For example, the shadowed region in Fig. 3.4 denotes the frequency range over which $\mu_{eff} < 0$ when $\Lambda = 0.2$. At these frequencies the values of Q^{rel} are not valid. Please note also that the width of the frequency range corresponding to $\mu_{eff} < 0$ is different when different amplitude factors are used.

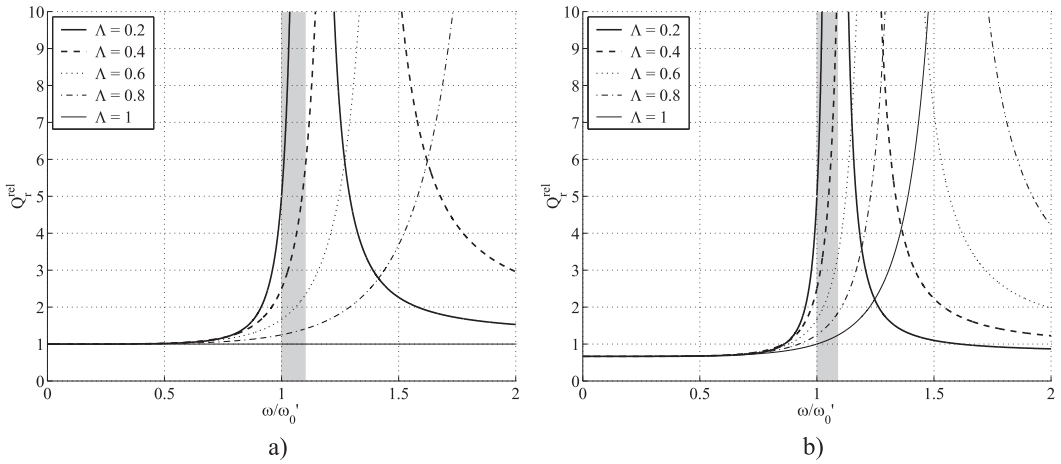

Figure 3.4: Relative radiation quality factors.

we have a system of coupled radiating resonators [55].

2) Composites containing thin iron sheets [$\mu_s = 1.5$ in (3.10)].

The result shown in Fig. 3.4b outlines an important fact: There exists a frequency band over which the effect of enhanced static permeability outweighs frequency dispersion. Only close to the substrate resonance the strong frequency dispersion dominates.

As a summary we conclude that also practically realizable magnetic substrates offer advantages in antenna miniaturization in terms of retained impedance bandwidth. However, the substrate must obey 1) static magnetic polarization, 2) weak frequency dispersion, and 3) at most moderate losses. It is interesting to note that the *static* properties of the magnetic substrate play a key role in the *microwave* performance of the antenna. Similar observation has been made earlier in connection with radar absorbers: According to the Rozanov limit [56] for the thickness to bandwidth ratio of radar absorbers, the thickness of the absorber at microwave frequencies (with a given reflectivity level) is bounded by the static permeability value of the absorber.

3.5 Review of related results found in the literature

Recently, there has been a flow of research devoted to antenna miniaturization using broken loop composites [**III**, **IV**], [55, 57–66]. The earlier numerical and experimental results [55, 57–65] do not, however, offer a complete, quantitative comparison scheme applicable for practical antenna design. The impedance bandwidths (quality factors) of reduced size antennas utilizing *practically realizable*, *dispersive* composite substrates have not been compared to the results obtained using high-permittivity dielectrics leading to the same size reduction. This quantitative comparison is clearly needed to make decisions whether or not the possibly enhanced impedance bandwidth outweighs the increased manufacturing cost and substrate weight [**III**, **IV**], [66].

Despite the progress in the manufacturing technology of ferrite materials, we still have to deal with the fact that natural magnetic materials either loose their magnetic properties or become too lossy for antenna applications at the current mobile communications frequencies. According to the author's knowledge, there are no results available for the use of antenna substrates possessing static magnetic polarization even in the lower GSM (Global System for Mobile Communications) band at 900 MHz, not to even mention higher frequencies. The limit for the feasible frequency range of ferrite based antenna substrates was mentioned to be 500 MHz in [67], also authors of [57, 64] considered 500 MHz as a limit for the feasible use of composites containing Z-type hexaferrite.

3.6 Contributions of this thesis (summary of related publications)

1. In [**III**] we introduce a complete, quantitative comparison between the radiation quality factors obtained using broken-loop composites and conventional dielectric substrates offering the same size reduction. Using a transmission-line method we first study the obtained impedance bandwidths. Later, an explicit relation is derived for the ratio between the radiation quality factors. All the results indicate that broken loop composites offer no advantages compared to conventional dielectrics in terms of more effectively retained impedance bandwidth. This result is experimentally validated.

2. In [**IV**] we review the main observations of [**III**], and further clarify the effect of static permeability and frequency dispersion on the impedance bandwidth characteristics. Moreover, detailed discussion is conducted on the available (feasible) magnetic substrates showing static magnetic polarization, and their effect on the achievable impedance bandwidth. We propose to use composites containing thin iron sheets as antenna substrates. Calculated and simulated results show that the proposed substrates outperform conventional dielectric substrates in terms of minimized radiation quality factor.

4 Capacitively loaded wire medium as a light-weight beam shaping element

4.1 Introduction

The transition era from the third generation systems to 4G networks leads to applications that will require huge data rates and therefore extremely efficient network planning [35, 68]. Undoubtedly, novel implementation techniques are needed to lighten the pressure concerning the improvement of base station antennas. Ultimately, the antenna must be robust and cheap for mass production implying that the structure should be small and simple. However, sectorized cells and the natural evolutional stages of the network often set the demand for the antenna to operate in different modes with different service areas. Therefore, the antenna should offer a possibility for a tunable beam width or a switchable beam direction. Incorporating intelligence in a miniaturized and simple antenna structure while still maintaining the efficiency high, is not an easy task.

In this chapter we consider the wire medium (introduced below in more details), and study the feasibility to utilize such an *artificial dielectric composite* as a material for a beam shaping element in base station antenna applications. We manipulate the dispersion properties of the wire medium by loading the wires with a certain distributed impedance. It will be demonstrated that a proper impedance loading makes the medium more feasible for use in antenna beam shaping. At frequencies where the structural dimensions are small compared to the wavelength the waves "see" the composite as a weakly dispersive homogeneous dielectric with a certain effective permittivity. In the related original publications [**V**, **VI**] we study how well a finite size lattice of loaded wires can be interpreted as a block of homogeneous dielectric material in terms of its beam shaping capability in the horizontal plane (H-plane).[9] The practical goal of the work [**V**, **VI**] is to design a compact dual-mode base station antenna having a mechanically reconfigurable beam width in the H-plane.

4.2 Wire medium: Review of some key features

4.2.1 Dispersion properties

Consider a periodical lattice of thin conducting wires, Fig. 4.1a. The wires are infinitely long, and the number of wires in X and Y-directions is infinite. We call such a structure *wire medium* (also the term *rodded medium* is sometimes used in the literature). Here we plan to utilize the structure at frequencies where the wavelength is much larger than the lattice constants, $a, b \ll \lambda$. At this frequency range the composite can be interpreted as an equivalent homogeneous material having some

[9] More precisely, horizontal plane in this context refers to the plane perpendicular to the wires.

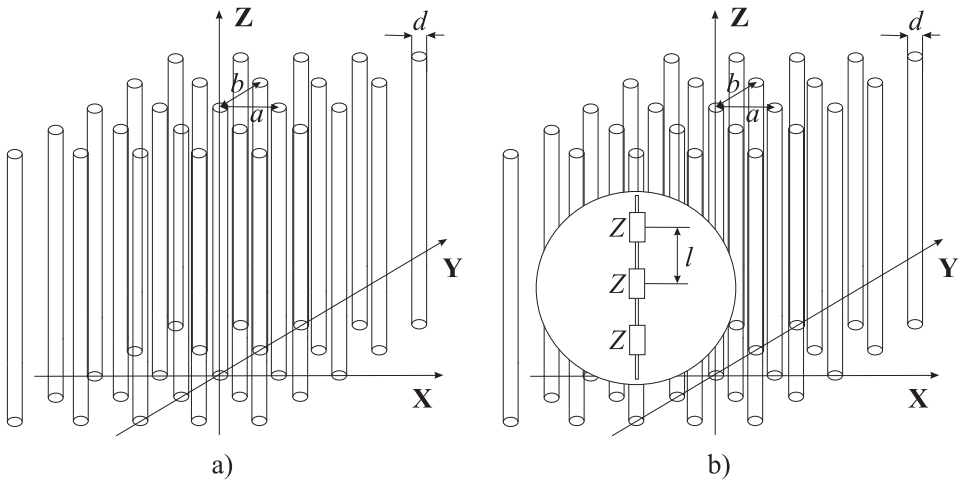

Figure 4.1: a) Artificial wire medium, b) loaded wire medium.

effective permittivity. To outline some important physical aspects derivable from the above mentioned assumption, we will briefly review the physics and assumptions behind the effective medium description.

Consider one grid of wires, e.g. the first grid in X-direction in Fig. 4.1a. Moreover, assume this grid to be excited by a plane wave so that its electric field has a component parallel to the wires. This field component induces currents in all the wires, and these currents produce an electric field which can be represented as a sum of different Floquet harmonics [1, Ch. 4]. The lowest-order harmonic represents a plane wave originating from the averaged current in the grid. The higher-order harmonics have a reactive nature and they decay exponentially as the observation point moves away from the grid plane. If the lattice constant b is small compared to the wavelength in free space (and compared to the wavelength of waves traveling along the grid), the contribution of the higher-order harmonics is small already at distance a away from the grid plane. Thus, the grid can be represented as an averaged current sheet, and many grids constituting the wire medium can be thought of as periodically arranged current sheets. In the quasi-static regime the theory of periodically loaded transmission lines [1, 69, 70] can therefore be used to understand the dispersion properties of the wire medium.

Consider now a transmission line periodically loaded (in parallel) with certain bulk impedances Z_{load}, the physical distance between the loads being a. The classical result for the dispersion equation (relation between the propagation factor along the line q and the frequency) of such a line reads [1, 69]

$$\cos qa = \cos ka + j\frac{\eta}{2Z_{\text{load}}}\sin ka, \tag{4.1}$$

where η is the wave impedance and k the wavenumber in the matrix (background medium). There are several detailed results available in the literature for the estimation of Z_{load} in case of different inclusions (e.g. metal wires) constituting artificial dielectrics, e.g. [69–72]. It is physically clear, however, that at low frequencies the wires can be represented as effective distributed inductances due to the induced current flowing in the wires. If Z_{load} is inductive in (4.1) the dispersion diagram shows a wide stop-band starting at zero frequency, e.g. [1]. This stop-band is physically understandable since at low frequencies the impedance level of an inductor is very low and the transmission line is effectively short circuited. In other words, when $a, b \ll \lambda$ the wave sees the grids of wires as metal walls. Qualitatively similar behavior is also seen when the dynamic dispersion equation for the wire medium is numerically solved [73].

Recently, an interesting modification was proposed for the wire medium: Authors of [74, 75] loaded the wires with reactive impedances in order to manipulate the dispersion properties of the medium, Fig. 4.1b. Here we call such a composite *loaded wire medium*. An interesting special case is the capacitive loading of the wires (e.g. slits are cut to the wires). In this case the load in the waveguide is a series connection of inductance (due to the wire segments) and capacitance (due to the slits). At low frequencies the impedance is strongly capacitive (the loads are nearly open circuits) and waves can propagate through the medium. Thus the low frequency stop-band inherent for conventional wire medium disappears (for an experimental observation of this phenomenon see [76]). When the load circuit is in resonance, there appears a stop-band because the impedance level tends ideally to zero (authors of [75] call this resonance *self resonance*). The dispersion diagrams for a capacitively loaded wire medium (obtained when the dynamic dispersion equation is numerically solved [75]) indicate that the wavenumber increases almost linearly as a function of frequency well enough below the first resonance of the medium. This means that the medium behaves effectively as an artificial dielectric with effective permittivity $\epsilon_{\text{eff}} > 1$ at these frequencies. It is also worth to note that at frequencies well below the resonance the currents induced to the wires are small in amplitude, thus, power losses in the artificial dielectric are very small.

As an illustrative special case authors of [73,75] considered TM-polarized plane waves traveling orthogonal to the unloaded and loaded wires. The dispersion equation, valid in the quasi-static regime, was reformulated using the resonant effective permittivity. For the conventional wire medium the effective permittivity reads [73,75]:

$$\epsilon_{\text{eff}} = 1 - \frac{k_{\text{p}}^2}{k^2}, \tag{4.2}$$

and for the capacitively loaded wire medium [75]:

$$\epsilon_{\text{eff}} = 1 + \frac{A k_{\text{p}}^2}{k_{\text{p}}^2 - k^2}, \quad A = \frac{C}{\epsilon_0 a b} \tag{4.3}$$

where k_{p} is the plasma wave number, k is the wavenumber in the matrix, and C

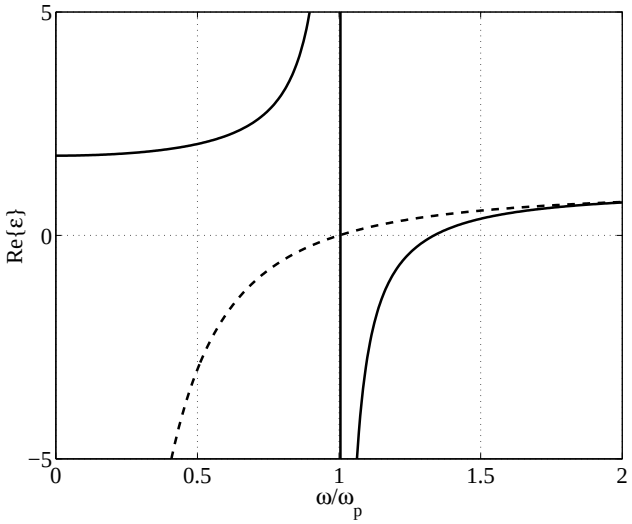

Figure 4.2: Real part of effective permittivity ϵ_{eff} of conventional wire medium (dashed line) and capacitively loaded wire medium (solid line) as a function of normalized frequency.

is the load capacitance per unit length. k_{p} is determined by the geometrical dimensions, and in the case of capacitively loaded wires, also by the load capacitance value [75]. A plot showing the effective permittivity of conventional and capacitively loaded wire medium is shown in Fig. 4.2 (the structural parameters and load capacitance have realistic values). We see that wave propagation through the conventional wire medium is prohibited below ω_{p}, whereas the capacitively loaded wire medium behaves as an artificial dielectric with $\epsilon_{\text{eff}} > 1$ at these low frequencies.

As a summary we conclude that capacitive loading adds two important features to the dispersion properties of the wire medium: 1) The low frequency stop-band inherent for conventional wire medium disappears and waves can propagate through the medium. 2) The capacitively loaded wire medium simulates the dispersion properties of a homogeneous dielectric material with $\epsilon_{\text{eff}} > 1$ at low frequencies.

Please note that the low frequency analysis outlined above is rather strongly simplified, as the goal has been only briefly outline some important features in order to understand the behavior of the composite with real antenna applications. An interested reader is reminded that there exist several sophisticated articles analyzing rigorously the dispersion properties of the wire medium (in addition to [73, 75], see e.g. [77–79]).

4.2.2 The effect of spatial dispersion

General

When the dynamic dispersion equation for the wire medium is rigorously derived (as e.g. in [73]) and cast in the form of (4.1), the equivalent load impedance Z_{load} is a complicated function and it depends on the wavevector components in the medium. In the physical domain this means that the impedance depends on the spatial derivatives of electromagnetic fields, thus, the wire medium is said to be spatially dispersive. Typically spatial dispersion refers to the fact that waves "feel" the details of the material or medium, i.e., such an effect is considered to be important when the structural dimensions are comparable to the wavelength [1, 16]. However, with wire medium the effect of spatial dispersion has been shown to be important also in the long-wavelength limit [80] (interesting discussion is also presented in [81] where the authors generalize the results of [80] for so called double and triple wire media). Indeed, if we want to model the composite as a homogeneous uniaxial dielectric (as is clear from the structural geometry), the effective permittivity has to be a non-local dyadic [80]:

$$\bar{\bar{\epsilon}}_{\text{eff}} = \epsilon_0 \bar{\bar{I}}_t + \epsilon_z \mathbf{z}_0 \mathbf{z}_0, \quad \epsilon_z = \epsilon_0 \left(1 - \frac{k_{\text{p}}^2}{k^2 - q_z^2} \right), \tag{4.4}$$

where $\bar{\bar{I}}_t$ is the tangential unit dyadic, $\mathbf{z}_0$ is a unit vector in the Z-direction (Fig. 4.1). $\epsilon_t = \epsilon_0$ because in the thin-wire assumption we neglect the transversal polarization of wires. When the propagation is normal to the wires, $q_z = 0$, and (4.4) reduces to (4.2).

The effect of spatial dispersion with wire medium antennas having finite height

When the wires are finite in height and excited by a realistic (finite length) closely located line source, spatial dispersion is clearly always present. A finite length line source (e.g. a dipole antenna) produces some harmonics which have propagation constant component parallel to the wires. A relevant question is if the effect of spatial dispersion is seen in the antenna radiation pattern.

Extensive preliminary simulations leading to the results presented in [**V**, **VI**] show the following: The height of wires in a finite size wire lattice has only a small effect on the radiation pattern in the H-plane (in the studied scenarios the height is always larger than λ). Therefore it is assumed that also the effect of spatial dispersion is not seen in the H-plane radiation pattern.

When the wires are infinitely long spatial dispersion affects the direction of radiation maximum in the vertical plane (E-plane), see e.g. [**VII**]. However, the author assumes that if the wires have a finite height, the standing wave patterns induced to the wires [82] "screen" the effect of spatial dispersion also in the E-plane radiation pattern.

4.2.3 Wire antenna inside the composite

At this stage we know how the wire medium behaves macroscopically at low frequencies with plane wave excitation. Since our ultimate goal is to utilize the capacitively loaded wire medium as a beam shaping element in antenna applications, let us see how the presence of wires, unloaded or loaded, affects the radiation characteristics (e.g. the radiation resistance) of the source. If the wires are thin and ideally conducting, the boundary condition at the surface of the wire closest to the source line reads (the distance between the source line and the reference wire is denoted R_s):

$$-\frac{\eta(k^2-q_z^2)}{4k}H_0^{(2)}(\sqrt{k^2-q_z^2}R_\mathrm{s})I_\mathrm{s}-\frac{\eta(k^2-q_z^2)}{4k}H_0^{(2)}(\sqrt{k^2-q_z^2}d/2)I^\mathrm{ind}+E_\mathrm{sum}=0, \tag{4.5}$$

where I_s is the amplitude of the source current, I^ind is the amplitude of the current induced to the reference wire, k is the wavenumber in the matrix, q_z is the wavevector component along the wires, and $H_0^{(2)}$ represents the Hankel function of the second kind and zero order. E_sum is the electric field at the surface of the reference wire produced by the currents induced in all the other wires (for more discussion how to derive (4.5), see e.g. [83]). In (4.5) the first term is the field created by the source line, and the second term is the field created by the current induced to the reference wire at its surface. If the source line is very close to the nearest wire, we can as a first approximation assume that the first term in (4.5) dominates over E_sum [84]. When we use the asymptotic formula for the Hankel function with a small argument the induced current can be expressed as a function of the source current in the following form [83, 84]

$$I^\mathrm{ind}\approx-\frac{\log\left[2/(\sqrt{k^2-q_z^2}R_\mathrm{s})\right]}{\log\left[4/(\sqrt{k^2-q_z^2}d)\right]}I_\mathrm{s}. \tag{4.6}$$

We notice that with the aforementioned assumptions the current induced in the closest wire will be out of phase with the source current (due to the minus sign), thus, the fields created by these two currents will add up destructively leading to poor radiation.

Similarly as in the previous subsection let us see what is the effect of capacitive loading. If the wires are loaded with bulk capacitors in a way that the insertion period for the loads is small compared to the wavelength, an incoming wave will "see" some impedance per unit length at the wire surface (for unloaded wires this impedance is zero). Further, the impedance loading changes the boundary condition (4.5) since now the total field at the wire surface can be represented as a product of the distributed impedance and the induced current [84]. With the above introduced assumptions the current induced to the closest wire takes the form (more details in [84])

$$I^\mathrm{ind}\approx\frac{k\eta|\alpha_z|\log[2/(\sqrt{k^2-q_z^2}R_\mathrm{s})}{2\pi}I_\mathrm{s}, \tag{4.7}$$

where η is the wave impedance in the matrix, and α_z is the susceptibility of the loaded wire [84]. We notice that in this case the fields created by the source current

and the current induced to the closest wire will add up in phase, thus, the loaded wires can be brought very close to the source while still maintaining the radiation efficiency (resistance) at a reasonably high level.

4.3 Capacitively loaded wire medium with antennas: Summary of important features

If we would like to utilize conventional wire medium as a beam shaping element at low frequencies, a channel would need to be configured in the structure to allow radiation. The wires should also be located rather far away from the source, as the currents induced to closely located unloaded wires will be out of phase with the source current. Thus, the transversal dimensions of the structure will inevitably be rather large (assuming that effective radiation characteristics are desired).

There are two important features which the capacitive loading offers:

1. We synthesize the dispersion properties of a conventional weakly dispersive dielectric material. This means that some of the well-known antenna design principles, such as the theory of an aperture radiator [42], for example, can be used when designing the beam shaping element. Since the macroscopic response is achieved with a sparse wire lattice, the proposed composite is extremely light-weight and cheap to manufacture. This is especially important at low frequencies where the dimensions of conventional microwave lenses can be rather large.

2. We can bring the loaded wires very close to the source line (antenna), and still maintain a reasonably high radiation resistance. Thus, we achieve an antenna structure which radiates effectively but whose transversal dimensions are simultaneously very compact.

4.4 Review of related results found in the literature

Already in the late 1940's Kock demonstrated that a periodical arrangement of metal plates or a mixture of electrically small polarizable inclusions shapes the beam of a low-gain radiator similarly as a solid dielectric lens having certain relative permittivity [85, 86]. During 1950's a lot of work was devoted to the development of artificial dielectrics for microwave applications, especially for lens antennas, see e.g. [69, 71] and the extensive reference lists therein. In the beginning of 1960's Rotman [72] and Golden [87] studied antenna beam shaping using conventional wire medium operating just above the plasma frequency. Similar frequency range has in the past also been studied in connection with leaky wave antennas, e.g. [88, 89].

More recently authors of [90, 91] studied the radiation characteristics of a dipole antenna illuminating a 3-D wire lattice (acting as a reflector). In [92–94] a channel

was constructed inside a lattice of unloaded wires, and the authors theoretically and experimentally studied the radiation properties of a dipole inside such a construction. Authors of [95] created a channel inside a wire lattice arranged in an elliptical geometry, and studied numerically and experimentally the radiation properties of a monopole inside such a construction. He and coauthors presented in [96, 97] an efficient method to obtain the radiation characteristics of a dipole antenna embedded inside 2-D and 3-D arrays of metal wires. The method of [96] was later used in [84] to study the radiation characteristics of an array of capacitively loaded wires illuminated by a closely located dipole. In [98] de Lustrac and coauthors presented an electromagnetic band-gap (EBG) structure consisting of cut metal strips mounted with pin-diodes. Depending on the diode biasing the structure was shown to prohibit the propagation of the electromagnetic waves or to create a very directed beam for a planar antenna. Note that already in the 1980's Milne [99] studied antenna beam shaping using an array of dipoles (this technique somewhat resembles the case of discontinuous wires with the introduced cap width extending towards infinity). In addition to the active antenna design presented in [94], the authors of [100] proposed to manipulate the radiation pattern of wire array antennas by using pin-diodes. Please note, however, that due to very high signal power levels used in base stations (e.g. Kathrein [101] reports the maximum power per input to be 300 W for most of the products), active components might not be feasible in the beam shaping element due to unavoidable intermodulation products leading to distorted frequency spectrum.

It is nowadays well understood (see e.g. [102–104]) that some electromagnetic crystals simulate the behavior of a homogeneous material with ultra-low refractive index just above the stop-band edge (this behavior is also seen in Fig. 4.2 for conventional wire medium). In [105] (see also [106]) the authors heuristically and experimentally demonstrated that a monopole source produces a highly directive beam when embedded inside a wire mesh operating at such a frequency (note that the same qualitative observation was made based on experimental results already in [72]). Recent analysis for (infinite) line source radiation inside the wire medium utilized in its super-refractive ($\epsilon_{\text{eff}} \approx 0$) regime can be found in [107, 108]. Conventional wire medium could possibly be utilized in antenna beam shaping also inside its low-frequency stop-band: It is known (e.g. [109]) that a slight local change in the photonic (equivalently electromagnetic) crystal period leads to localized resonant modes, and can be used for the realization of devices radiating energy in a very narrow angular range. For example, authors of [110,111] demonstrated the feasibility of this concept in directive antenna design using arrays of dielectric rods, and authors of [112] used stacked dielectric plates. An idea to control the wire crystal resonances by using different row periods was proposed in connection with dual-band directive antennas in [113].

4.5 Contributions of this thesis (summary of related publications)

1. In [**V**, **VI**] we propose a new technique to utilize the wire medium as a beam shaping element. The key idea is to load the wires capacitively so that we can utilize the medium at low frequencies where the loaded medium has a pass-band. Moreover, at low frequencies such a composite effectively behaves as a weakly dispersive homogeneous dielectric with $\epsilon_{\text{eff}} > 1$, thus, conventional lens antenna design rules can be qualitatively applied. No resonant phenomenon is incorporated in the beam shaping mechanism, thus, the beam shaping element is wide-band and has low losses. Moreover, by changing the values of capacitive loads the effective permittivity of the beam shaping element can be altered.

   From the practical point of view we design and implement base station antenna prototypes operating in the Universal Mobile Telecommunication System (UMTS) frequency band [**VI**]. It is shown that in terms of H-plane beam shaping, the interpretation of a finite-size wire lattice as a homogeneous dielectric block is physically sound even in the presence of only a moderate number of wires. The designed prototypes are simple and cheap to manufacture and they show promising performance.

5 Vector circuit theory for spatially dispersive uniaxial magneto-dielectric slabs

5.1 Motivation

5.1.1 General

Consider the slab shown in Fig. 5.1a. The slab is implemented using a periodical arrangement of metal wires and broken loops, and is illuminated by a TM-polarized plane wave (periodical arrangements of the aforementioned inclusions have already been studied earlier in this thesis). During the recent few years, followed by the popularization of the *metamaterial* concept [114–116], the aforementioned structure has faced immense amount of studies. This is largely due to the fact that the structure was used in the first realization of so called double-negative medium (DNG) [117, 118]. The number of articles analyzing the structure in Fig. 5.1a is big and rapidly growing (for some rather early contributions, see e.g. [119–121]).

For this work the interest in the wire array / broken-loop structure arises from recent practical suggestions to utilize slabs with ultra-low refractive index in microwave applications: We know that electromagnetic crystals simulate the behavior of a homogeneous material with ultra-low refractive index just above the stop-band edge [102–104]. This behavior is clearly seen also in Fig. 4.2 where we observe that for the conventional wire medium $\epsilon_{\text{eff}} \approx 0$ just above the plasma frequency. In addi-

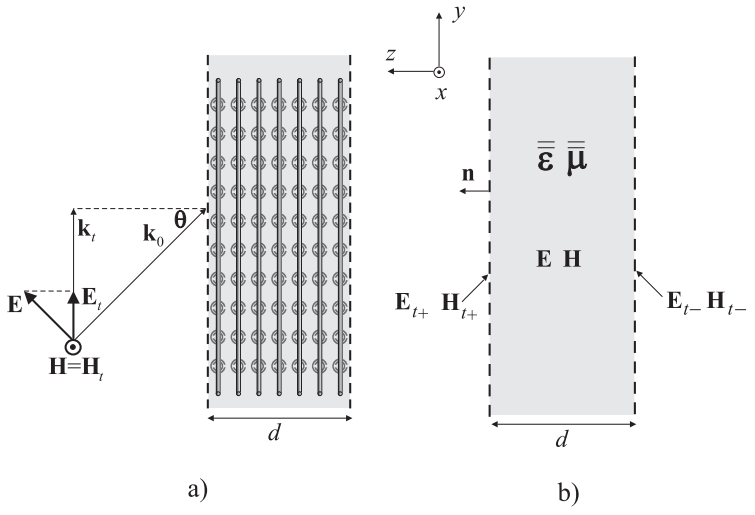

Figure 5.1: TM-polarized plane wave incident on a slab implemented using wires and broken loops.

tion to this, the dispersion analysis of composites consisting of broken loops (please see Fig. 2.3) also indicates that the effective permeability μ_{eff} of such composites has a very low value above the first resonance. Slabs having ultra-low refractive index have been proposed to enhance the directivity of antennas [72, 105–108]. In addition to this, the aforementioned slabs have been proposed to reduce reflections from waveguide bends [122, 123].

At frequencies where the wavelength is large compared to the inclusion dimensions and their spacing the structure in Fig. 5.1a can apparently be described as a uniaxial magneto-dielectric slab, Fig. 5.1b. Moreover, as is clear from the discussion in the previous chapter, the presence of wires imposes strong spatial dispersion also in the long-wavelength limit. However, in many works devoted to wave interaction with metamaterials the material is assumed to be isotropic and characterized by local material parameters (see e.g. [124–129]), even though the authors often mention that a practical implementation of the material corresponds to the structure in Fig. 5.1a. For example, authors of [128] consider slabs having ultra-low refractive index and explicitly mention that in reality the slab (implemented using wires and broken loops) would be uniaxial, however, the analysis is carried out for isotropic and local slabs.

5.1.2 Earlier works

It is well known that many problems dealing with reflections from multilayered media can be solved using the transmission-line analogy when the eigen-polarizations are studied separately (see e.g. [130]). In this case, the amplitudes of tangential electric and magnetic fields are treated as equivalent *scalar* voltages and currents in the equivalent transmission-line section. In order to account for an arbitrary polarization, Lindell and Alanen introduced a *vector* transmission-line analogy [131], where *vector* tangential electric and magnetic fields serve as equivalent voltage and current quantities. Later on, the vector transmission-line analogy was further extended for isotropic and chiral slabs into a vector circuit formalism, with the slabs represented as two-port circuits with equivalent dyadic impedances and admittances [132]. This vector circuit theory has been successfully applied to study wave propagation in chiral slab waveguides [133], and plane wave reflection from chiral slabs [134]. It has also been extended to uniaxial multilayer structures [16, 135].

5.2 Example: Reflection and transmission coefficient for a TM-polarized plane wave using the proposed method

Let us briefly illustrate the usability of the proposed method. Consider the TM-scattering scenario depicted in Fig. 5.1a and assume that the incident wave vector is restricted to the yz-plane. At the macroscopic level (Fig. 5.1b) the slab consisting of broken loops and long conductors can be represented using the following effective

material parameter dyadics:

$$\overline{\overline{\epsilon}} = \epsilon_t(k_t)\overline{\overline{I}}_t + \epsilon_n \mathbf{nn}, \quad \overline{\overline{\mu}} = \mu_t\overline{\overline{I}}_t + \mu_n \mathbf{nn}, \tag{5.1}$$

where $\mathbf{n}$ is the unit normal vector for the slab, and $\overline{\overline{I}}_t = \overline{\overline{I}} - \mathbf{nn}$ is the transversal unit dyadic. Notation $\epsilon(k_t)$ stresses the spatially dispersive nature of the slab in the tangential plane, and indicates the dependence of the permittivity component on the tangential propagation factor (please see the discussion related to the spatially dispersive nature of the wire medium in the previous chapter). The tangential field amplitudes at both interfaces of the above described slab (Fig. 5.1b) can be solved and cast in the following form (detailed derivation is available in [**VII**]):

$$\begin{pmatrix} \mathbf{E}_{t+} \\ \mathbf{n} \times \mathbf{H}_{t+} \end{pmatrix} = \begin{pmatrix} \alpha_{11} & \alpha_{12} \\ \alpha_{21} & \alpha_{22} \end{pmatrix} \begin{pmatrix} \mathbf{E}_{t-} \\ \mathbf{n} \times \mathbf{H}_{t-} \end{pmatrix}, \tag{5.2}$$

where the transmission components read for TM-incidence:

$$\alpha_{11} = \alpha_{22} = \cos(\beta_{\mathsf{TM}} d), \tag{5.3}$$

$$\alpha_{21} = j\frac{\omega\epsilon_t(k_t)}{\beta_{\mathsf{TM}}}\sin(\beta_{\mathsf{TM}} d), \tag{5.4}$$

$$\alpha_{12} = j\frac{\beta_{\mathsf{TM}}}{\omega\epsilon_t(k_t)}\sin(\beta_{\mathsf{TM}} d), \tag{5.5}$$

where the propagation constant for TM-polarized waves reads

$$\beta_{\mathsf{TM}} = \sqrt{\frac{\epsilon_t(k_t)}{\epsilon_n}(\omega^2\mu_t\epsilon_n - k_t^2)}. \tag{5.6}$$

Following the treatment in [1,131,132] we interpret $\mathbf{E}_{t+}$ as *vector* input voltage and $\mathbf{n} \times \mathbf{H}_{t+}$ as *vector* input current. Using this interpretation the matrix in (5.2) is the transmission matrix of the slab. After this identification the plane-wave transmission and reflection coefficients T, R can be straightforwardly solved after writing (5.2) as a system of two equations with two unknowns [**VII**]:

$$T = \frac{2}{\alpha_{11} + \alpha_{22} + \alpha_{12}/Z_0 + \alpha_{21}Z_0}, \tag{5.7}$$

$$R = (\alpha_{11} + \alpha_{12}/Z_0)T - 1, \tag{5.8}$$

where $Z_0 = \eta_0 \cos\theta$ is the free space wave impedance seen by the tangential fields.

For the specific case shown in Fig. 5.1a the non-local permittivity dyadic reads (the notation is clear from the previous chapter):

$$\overline{\overline{\epsilon}} = \epsilon_x \mathbf{u}_x\mathbf{u}_x + \epsilon_y \mathbf{u}_y\mathbf{u}_y + \epsilon_z \mathbf{u}_z\mathbf{u}_z, \tag{5.9}$$

$$\epsilon_x = \epsilon_z = \epsilon_\mathrm{h}, \quad \epsilon_y = \epsilon_\mathrm{h}\left(1 - \frac{k_\mathrm{p}^2}{k^2 - q_y^2}\right), \tag{5.10}$$

where ϵ_h is the permittivity of the host matrix. The permeability dyadic reads (here we assume that the host matrix is lossless, the notation is clear from Chapter 2):

$$\overline{\overline{\mu}} = \mu_x \mathbf{u}_x \mathbf{u}_x + \mu_y \mathbf{u}_y \mathbf{u}_y + \mu_z \mathbf{u}_z \mathbf{u}_z, \tag{5.11}$$

$$\mu_x = \mu_\mathrm{h}\left(1 + \frac{A\omega^2}{\omega_0^2 - \omega^2 + j\omega\Gamma}\right), \quad \mu_y = \mu_z = \mu_\mathrm{h}, \tag{5.12}$$

where μ_h is the permeability of the host matrix. For an example analysis we assume the following parameters: Slab thickness $d = 150$ mm, $\epsilon_\mathrm{h} = \epsilon_0$, and $k_\mathrm{p} = 104.7$ m^{-1} (the corresponding plasma frequency is $f_\mathrm{p} = 5$ GHz); $\mu_\mathrm{h} = \mu_0, A = 0.4, \omega_0 = 2\pi \cdot 2.5 \cdot 10^9$ rad/s, $\Gamma = \omega_0/50$.

We compare the transmission coefficient, calculated when the uniaxial and spatially dispersive nature of the slab is taken into account, to the result obtained when the slab is assumed to be isotropic and local[10] (as mentioned earlier, this is a rather common assumption when analyzing wire array / broken loop slabs). The comparison is depicted in Fig. 5.2 [**VII**]. Clearly the assumption that the slab is isotropic and local leads to severe errors when estimating the transmission level, except for the normal incidence.

[10] In this case $q_y = 0$ in (5.10).

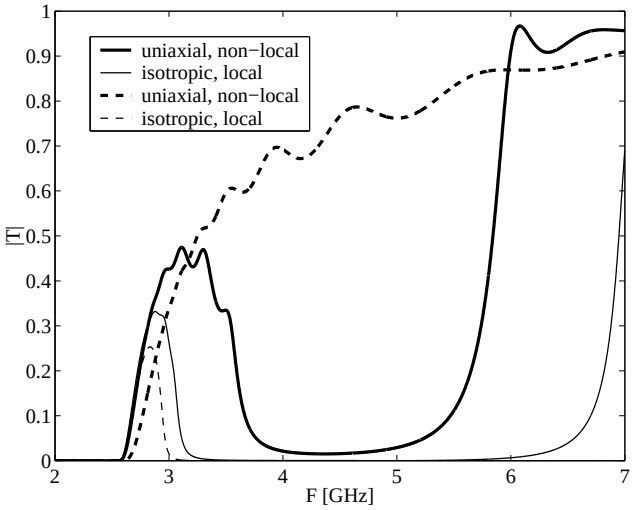

Figure 5.2: Transmission coefficient (absolute value) as a function of frequency at different incidence angles. Exact transmission coefficient (thick lines) is compared to the transmission coefficient calculated using local and isotropic permittivity model (thin lines). Solid lines: $\theta = \pi/6$, dashed lines: $\theta = \pi/3$.

5.3 Contributions of this thesis (summary of a related publication)

1. The purpose of [**VII**] is to extend the vector circuit formalism for uniaxial magneto-dielectric slabs, with strong spatial dispersion explicitly taken into account. Our goal is to come up with compact, yet exact expressions that allow to study transmission through slabs implemented using periodically arranged wires and/or broken loops with arbitrary plane wave incidence.

   We start from Maxwell's equations and solve the tangential field amplitudes at both interfaces of a general, spatially dispersive (in the tangential plane) uniaxial magneto-dielectric slab. No restriction is set for the incidence angle, or the polarization of the incoming plane wave. The aforementioned field expressions are used to construct two-port circuit expressions for the slab, and derive plane-wave reflection and transmission dyadics. Further, we consider practically realizable uniaxial magneto-dielectric slabs and calculate some example results for wave transmission through these slabs. The exact results are shown to differ noticeably from the results obtained when the spatially dispersive and uniaxial nature of the slab is neglected.

6 On sub-wavelength field channeling

6.1 Motivation and background

During the heyday of metamaterials [114–116] research concerning artificial electromagnetic media with extraordinary properties has increased explosively. Implementation of composites simulating the dispersion behavior of homogeneous materials having negative effective refractive index [117] has lead to the reconsideration of some of the most fundamental laws in physics [118]. It was shown in 2000 [136] that a slab having effective refractive index $n_{\text{eff}} = -1$ can bring a point source to a focus without aberration. Followed by this provocative "perfect lens" concept, one of the most extensively studied phenomena (relating to matematerials) has been *sub-wavelength imaging*. With such imaging we mean the transfer of the source field distribution into the far-zone (of the source) without losing the details of the distribution. To better understand the physics behind sub-wavelength imaging, and the bright ideas behind the proposed method, we will in the following briefly outline the origin for the resolution limit in conventional lenses.

6.1.1 Resolution limit in conventional lenses

Any field distribution (solution to the Helmholtz equation) can be expressed as a linear superposition of different (plane wave) harmonics (see e.g. [9]):

$$\mathbf{E}(\mathbf{r}) = \sum_n A(\mathbf{k}_n) e^{-j\mathbf{k}_n \cdot \mathbf{r}}, \tag{6.1}$$

where $\mathbf{r}$ is the spatial coordinate and $A(\mathbf{k}_n)$ is the amplitude of the harmonic having wave vector $\mathbf{k}_n$. Let us assume that electric field (6.1) is produced by a line source lying along y-direction in the cartesian coordinate system. For the sake of clarity it is for the following enough to observe that the plane wave harmonics of the electric field in this case are proportional to $e^{-jk_x x} e^{-jk_z z}$, i.e., the electric field consists of a continuum of harmonics $e^{-jk_x x} e^{-jk_z z}$. For illustration, the two dimensional electric field distribution of the line source is schematically shown in Fig. 6.1. The darker the shadowed region is, the stronger is the amplitude of the field (the singularity at the line source location is not plotted). Let us assume that the harmonics propagate in the z-direction (we could e.g. imagine that somewhere along the z-axis is a lens). The z-component of the propagation constant can be written as follows:

$$k_z = \sqrt{k^2 - k_x^2}, \quad k^2 \geq k_x^2, \tag{6.2}$$

$$k_z = -j\sqrt{k_x^2 - k^2}, \quad k^2 < k_x^2. \tag{6.3}$$

From the above formulae we notice that the spatial spectrum of the source consists of *propagating* [eq. (6.2)] and *evanescent* [eq. (6.3)] harmonics. The resolution limit for conventional lenses arises explicitly from (6.3): The evanescent harmonics decay

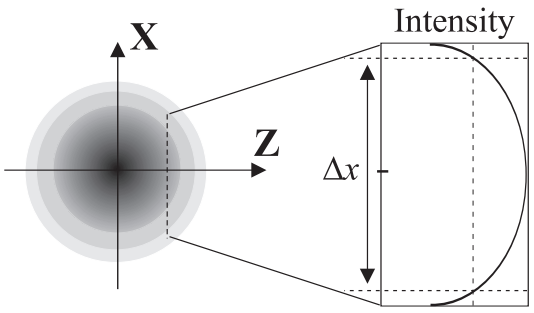

Figure 6.1: Schematic illustration of the electric field distribution produced by a line source oriented in y-direction. The electric field distribution is shown as the shadowed region (dark shadow = strong field).

exponentially as they propagate along z-direction. If we plan to put a lens at a certain distance (far enough) on the z-axis, the evanescent harmonics (amplitudes) have already decayed before they reach the lens. Thus, the evanescent part of the spectrum is effectively removed from the image formed behind the lens. If we think about the transverse image resolution, only transverse wave numbers in the interval $0 \leq |k_x| \leq k_{\max} = k$ contribute to the image. The maximum "resolution" in this case is $\Delta x \sim 2\pi/k_{\max} = \lambda$ [9].

A typical plot of the intensity[11] distribution near the line source is shown in the right part of Fig. 6.1 (we can e.g. imagine that the intensity distribution has been measured in x-direction along the dashed line). Close to the source the evanescent waves have still not experienced strong decay, and the spectrum in the wave vector domain is still wide ($\Delta k = 0...k_{\max} > k$). Through the Fourier transform relation this wide spectrum produces a narrow spatial spectrum, and the "resolution" is less than free-space wavelength ($\Delta x < \lambda$). Such a resolution is called *sub-wavelength resolution*.

6.2 Sub-wavelength field channeling: Key ideas and related results found in the literature

To realize (an ideal) Pendry's "perfect lens", one has to implement a slab having effective refractive index $n_{\text{eff}} = -1$ [136]. In this case the slab is 1) matched to free space space, 2) the propagating harmonics will refract negatively at the slab interfaces, and 3) the evanescent harmonics experience resonant amplification at the interfaces due to surface mode excitation. Thus, negative refraction, and surface mode (plasmon) excitation are needed to implement the "perfect lens" proposed by Pendry. The number of articles devoted to the realization of the "perfect lens", or

[11] Following the definition in [9] the squared amplitude of electric field.

other devices capable of sub-wavelength imaging is big and rapidly growing. In the following we will only review the key ideas of the concept proposed in this thesis. A reader interested in details of other methods is advised to see the web-page of Prof. D. R. Smith for an extensive reference list of recent and widely cited corresponding papers [137].

It was theoretically shown by Notomi [138] and experimentally proven by Parimi and co-authors [139] that in photonic crystals (PC) or electromagnetic crystals (EC) negative refraction can be achieved at frequencies close to the electromagnetic band-gap edges. Luo and co-authors introduced a flat *superlens* formed by a slab of PC in [140], and studied theoretically the possibility for sub-wavelength imaging in a layer of EC [141]. Recently, it has been shown that with PC/EC based structures neither negative refraction nor surface plasmon excitation is required to obtain a point source image whose diameter is smaller than λ. In this case the sub-wavelength image size has theoretically been achieved when the crystal iso-frequency contour has a special (flat) shape [2, 142–145]. This phenomenon is here called *sub-wavelength field channeling* [2] (note that authors of [2] originally called this phenomenon *sub-wavelength image canalization*). This regime for sub-wavelength field channeling has been called in the literature as *self collimation* [142], *directed diffraction* [143], *tunneling* [144], *absolute negative refraction* [145], and *self-guiding* [146].

In sub-wavelength field channeling the crystal slab effectively operates as a transmission device transferring the near field distribution of a source from the front interface to the back interface. It is conceptually important to note that the slab is not a lens in the optical point of view, and that no focusing is incorporated to the phenomenon. When the slab operates within the channeling regime and the source is located close to the front interface, the evanescent free-space harmonics transform into propagating crystal eigenmodes at the first crystal interface [2] (see Fig. 4 and the explanation below it in [2]). The near field distribution of the source is carried by these eigenmodes to the back interface where it diffracts into the free space (the second crystal interface can be thought as an aperture radiator with the channeled near field distribution corresponding to the aperture distribution [147]). Very close to the back interface the channeled distribution can be detected.

The crystal structures used to theoretically demonstrate the sub-wavelength field channeling include lattices of dielectric rods [142, 144] and lattices of metal rods coated with high-permittivity dielectrics [145]. We propose to utilize capacitively loaded wire medium [75] for implementing the operational regime. Compared to conventional wire medium [78] or lattices of dielectric rods, capacitively loaded wire medium offers additional features which make it superior in design. Authors of [75] have shown that capacitively loaded wire medium has a band-gap near the resonant frequency of a single capacitively loaded wire (the so called *resonant band-gap*). By changing the value of the load capacitance, the location of this band-gap can be conveniently tuned. Moreover, high value of capacitance allows to locate the resonant band-gap significantly below the first lattice resonance, thus the needed regime can be achieved with an electrically dense lattice. The details of the channeled

distribution are restricted by the lattice period, because the smaller is the lattice period the larger is the restored (maximum) wave vector component. Thus, the more (electrically) dense is the lattice, the finer can be the details of the channeled distribution.

Alternative technique to implement the channeling regime at microwave frequencies

The original idea of sub-wavelength field channeling was based on the flat iso-frequency contour of capacitively loaded wire medium, utilized so that the incident wave vector is perpendicular to the wires [2]. The experimental demonstration presented here follows this initial design strategy. However, as speculated at the end of [2], the transmission-line modes of the wire medium [80] can be used to implement iso-frequency contours that are flat for any transversal wave vector component (please note that the capacitively loaded wire medium, when utilized as proposed in [2], can only be used to approximate this condition). An experimental demonstration of field channeling based on the wire medium transmission-line modes is presented in [148] (ref. [148] was published in the same issue of Physical Review B as [**VIII**]).

6.3 Implemented prototype and key results

A photograph showing the implemented channeling device is depicted in Fig. 6.2. The capacitively loaded wires have been implemented as loaded thin strips printed

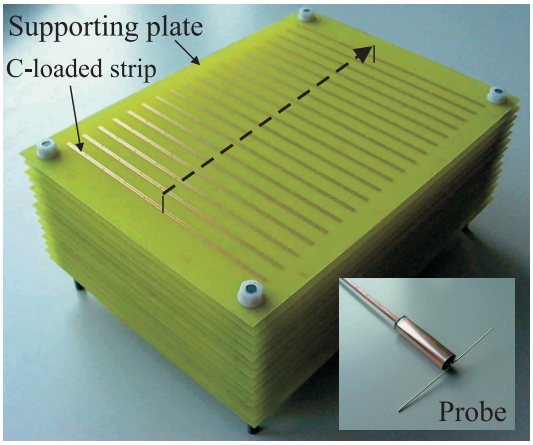

Figure 6.2: The implemented channeling device and one of the probes used in the measurements. The dashed arrow on top of the channeling devise indicates the measurement path in the channeling field area, corresponding to results shown in Fig. 6.3.

on dielectric FR4-plates. The total thickness of the implemented slab is 0.6λ at the operational frequency. Two probes based on resonant dipoles have been used to excite the structure and detect the field, please see the inset of Fig. 6.2.

One of the measured results [**VIII**] is depicted in Fig. 6.2. The intensity distributions in the channeled field (image) area have been measured at a 10 mm distance above the device output interface. The measurement path in the channeled field area is shown as the dashed arrow in Fig. 6.2. Intensity in the source area has been measured at a 10 mm distance from the source (the path is similar to the one used in the channeled field area). Before quantitatively analyzing the intensity distributions, we note that the measured intensity maximum occurs at the 10 mm distance above the interface (Fig. 6a in [**VIII**]), not right at the interface as predicted by the theory [2]. This shifting effect, often observed in the measurements, is elegantly explained in [149] by regarding the imaging slab as a matching device for the two antennas (the source and the detector). When the transmission coefficient for the above described system is solved using the impedance matrix formalism, one observes that a certain relation between the characteristic impedance of a single probe and the mutual impedance between the probes has to be fulfilled in order to obtain a transmission maximum (equivalently, an intensity maximum). Most likely such a condition is fulfilled with our setup when the probe is not exactly at the device interface (please see also the corresponding explanation in [**VIII**]).

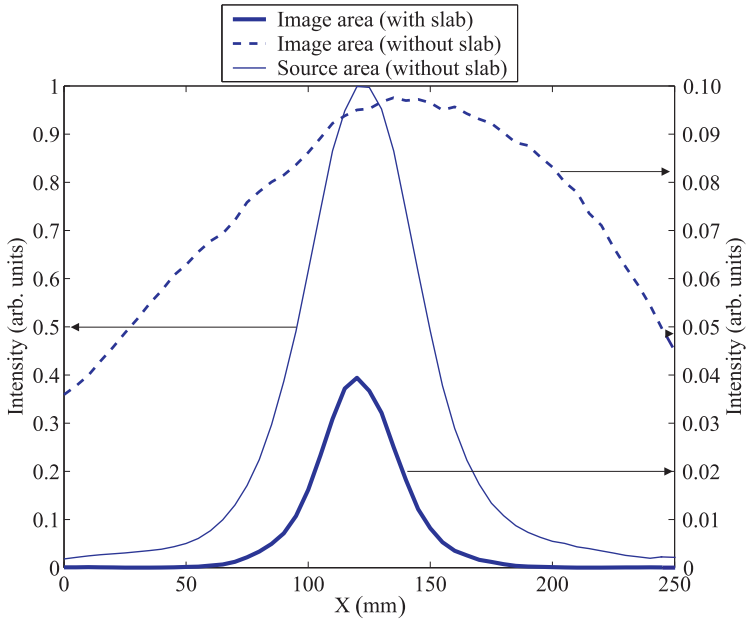

Figure 6.3: Measured intensity distribution. The measurement path in the channeled field area is shown as the dashed arrow in Fig. 6.2. The arrows indicate the scale which is used to read the intensity values.

When the channeling device is used in between the antennas we observe that the shape of the intensity distribution closely resembles the distribution in the source area. The maximum field value is approximately 35 % lower when using the channeling device than in the free space measurement. The main reason for this degradation is the strong reflection occurring at the first slab interface. The lossy dielectric plates also degrade the amplitude level of the channeled field. It is important to note, however, that the details of the distribution are not affected by the losses: The diameter of the intensity maximum (defined at level max(intensity)/2) is still roughly $\lambda/5$ when the channeling device is used. This important practical property is inherent to the subwavelength field channeling: The propagating waves in a lossy material experience the same decay irrespective of their transversal wave vector components, which are responsible for the shape of the channeled field distribution.

6.4 Contributions of this thesis (summary of a related publication)

1. In [**VIII**] we experimentally validate the theoretical results of [2]. A channeling device is implemented using a finite thickness slab made of capacitively loaded strips simulating the behavior of capacitively loaded wires. The measurement setup is carefully described and we measure 2-D and 1-D field distributions in the source and channeled field area. Using the implemented channeling device we obtain a channeled field distribution having diameter $\lambda/5$ at a distance $\lambda/1.4$ from the source. Without the slab the "resolution" at the same distance is roughly λ. Moreover, the experimental results of [**VIII**] demonstrate that losses in the slab do not affect the details of the channeled field distribution, they only degrade the amplitude of the channeled field.

7 Conclusions

In this thesis we have studied the performance enhancement of selected microwave applications using artificial electromagnetic composite structures. By combining two materials, e.g. by embedding metal inclusions in a dielectric matrix, it is possible to artificially synthesize a wide variety of macroscopic material properties. Special interest has been devoted to structures possessing artificial paramagnetic and artificial dielectric responses.

First, the fundamental properties of composites consisting of broken loops have been studied. A new artificial magnetic composite has been designed, implemented, and tested. Compared to the earlier designs the proposed design has several practical advantages. For example, the magnetic response has been strengthened with a stacked structure. Discussion has been addressed to the difficulties in defining stored electromagnetic energy and dissipated power in lossy artificial magnetic composites. As a result of this discussion, generalizations have been proposed to microscopic circuit model, macroscopic permeability function, and field energy density expression, commonly used to model these composites in the quasi-static regime.

Further, the applicability to use artificial magnetic composites as substrates for microstrip antennas has been studied. Composites consisting of thin iron sheets, also categorized into the class of artificial magnetic composites, have been briefly introduced for the same purpose. The goal has been to study if the proposed substrates offer any advantages in antenna miniaturization in the view of retained impedance bandwidth. For example, explicit expression has been derived for the ratio of radiation quality factors obtained using the proposed substrates and conventional dielectric substrates. The results indicate that in order to gain advantages the substrate must show static magnetic polarization, weak frequency dispersion, and at most moderate losses.

Artificial wire medium and loaded wire medium, categorized in the class of artificial dielectric composites, have been studied as a new artificial material for antenna beam shaping elements. The dispersion properties of the proposed composites have been reviewed in the quasi-static regime, and the effect of wires to the radiation characteristics of simple wire radiators has been discussed. State-of-the-art base station antenna prototypes utilizing the proposed beam shaping element have been designed, implemented, and tested. The prototypes are light-weight, simple and cheap to manufacture, and they show well predictable and promising performance.

A generalization has been proposed to the vector circuit theory, previously introduced for chiral and isotropic slabs. The proposed generalization applies to uniaxial magneto-dielectric slabs obeying strong spatial dispersion in the tangential plane. As a result of this extension to the theory, we can study the exact reflection and transmission through slabs implemented using periodically arranged metal wires and broken loops with arbitrary plane wave incidence.

Finally, in this thesis we have experimentally validated the theory of sub-wavelength field channeling. A near field channeling device operating in the microwave regime has been implemented using a lattice of capacitively loaded wires. This device is capable of transferring the details of the source distribution from one plane to another without losing the details of the distribution. The experimental setup has been described in details, and the results have been carefully analyzed. According to the author's knowledge the reported experimental result is one of the best results (in the view of finest resolution) reported at the time when this book is written.

References

[1] S. A. Tretyakov, *Analytical modeling in applied electromagnetics*. Norwood, MA: Artech House, 2003.

[2] P. Belov, C. Simovski, and P. Ikonen, "Canalization of sub-wavelength images by electromagnetic crystals," *Phys. Rev. B*, vol. 71, p. 193105, 2005.

[3] Y. T. Lo and S. W. Lee, Eds., *Antenna handbook: Theory, analysis and design*. New York: Van Nostrand Reinold, 1988, Chapter 7.

[4] R. Marqués, F. Medina, and R. Rafii-El-Idrissi, "Role of bianisotropy in negative permeability and left-handed metamaterials," *Phys. Rev. B*, vol. 65, p. 1444401, 2002.

[5] M. C. K. Wiltshire, J. V. Hajnal, J. B. Pendry, D. J. Edwards, and C. J. Stevens, "Metamaterial endoscope for magnetic field transfer: Near field imaging with magnetic wires," *Optics Express*, vol. 11, no. 7, pp. 709–715, 2003.

[6] A. Sihvola, *Electromagnetic mixing formulas and applications*. London: IEE Electromagnetic Wave Series, 1999.

[7] L. D. Landau and E. M. Lifshitz, *Electrodynamics of continuous media*, 2nd ed. Oxford, England: Pergamon Press, 1984.

[8] L. A. Vainstein, *Electromagnetic waves*, 2nd ed. Moscow: Radio i Sviaz, 1988 (in Russian).

[9] J. D. Jackson, *Classical electrodynamics*, 3rd ed. New York: John Wiley & Sons, 1999.

[10] T. J. Cui and J. A. Kong, "Time-domain electromagnetic energy in a frequency-dispersive left-handed medium," *Phys. Rev. B*, vol. 70, p. 205106, 2004.

[11] A. D. Boardman and K. Marinov, "Electromagnetic energy in a dispersive metamaterial," *Phys. Rev. B*, vol. 73, p. 165110, 2006.

[12] S. A. Tretyakov, "Electromagnetic field energy density in artificial microwave materials with strong dispersion and loss," *Phys. Lett. A*, vol. 343, pp. 231–237, 2005.

[13] S. A. Schelkunoff and H. T. Friis, *Antennas: Theory and practise*. New York: John Wiley & Sons, 1952.

[14] W. N. Hardy and L. A. Whitehead, "Split-ring resonator for use in magnetic resonance from 200–2000 MHz," *Rev. Sci. Instrum.*, vol. 52, no. 2, pp. 213–216, 1981.

[15] I. V. Lindell, A. H. Sihvola, S. A. Tretyakov, and A. J. Viitanen, *Electromagnetic waves in chiral and bi-isotropic media*. Norwood, MA: Artech House, 1994.

[16] A. Serdyukov, I. Semchenko, S. Tretyakov, and A. Sihvola, *Electromagnetics of bi-anisotropic materials: Theory and applications*. Amsterdam: Gordon and Breach Science Publishers, 2001.

[17] M. V. Kostin and V. V. Shevchenko, "Theory of artificial magnetic substrates based on ring currents," *Sov. J. Commun. Technol. Electronics*, vol. 38, no. 5, pp. 72–83, 1993.

[18] ——, "Artificial magnetics based on circular film elements," in *Proc. Bianisotropics'93*, Comel, Belarus, Oct. 12–14, 1993, pp. 32–35.

[19] ——, "Artificial magnetics based on double circular elements," in *Proc. Bianisotropics'94*, Périgueux, France, May 18–20, 1994, pp. 49–56.

[20] J. B. Pendry, A. J. Holden, D. J. Robbins, and W. J. Stewart, "Magnetism from conductors and enhanced nonlinear phenomena," *IEEE Trans. Microw. Theory Tech.*, vol. 47, no. 11, pp. 2075–2084, 1999.

[21] P. Gay-Balmaz and O. J. F. Martin, "Electromagnetic resonances in individual and coupled split-ring resonators," *J. Appl. Phys.*, vol. 92, no. 5, pp. 2929–2936, 2002.

[22] M. Shamonin, E. Shamonina, V. Kalinin, and L. Solymar, "Resonant frequencies of a split-ring resonator: Analytical solutions and numerical simulations," *Microwave Opt. Technol. Lett.*, vol. 44, no. 2, pp. 133–136, 2005.

[23] B. Sauviac, C. R. Simovski, and S. A. Tretyakov, "Double split-ring resonators: Analytical modeling and numerical simulations," *Electromagnetics*, vol. 24, pp. 317–338, 2004.

[24] R. Marqués, F. M. J. Martel, and F. Medina, "Comparative analysis of edge- and broadside-coupled split ring resonators for metamaterial design – theory and experiments," *IEEE Trans. Antennas Propag.*, vol. 51, no. 10, pp. 2572–2581, 2003.

[25] A. N. Lagarkov, V. N. Semenenko, V. N. Kisel, and V. A. Chistyaev, "Development and simulation of microwave artificial magnetic composites utilizing nonmagnetic inclusions," *J. Magnetism and Magnetic Materials*, vol. 258–259, pp. 161–166, 2003.

[26] J. D. Baena, R. Marqués, F. Medina, and J. Martel, "Artificial magnetic metamaterial design by using spiral resonators," *Phys. Rev. B*, vol. 69, p. 014402, 2004.

[27] M. Shamonin, E. Shamonina, V. Kalinin, and L. Solymar, "Properties of a metamaterial element: Analytical solutions and numerical simulations for a singly split double ring," *J. Appl. Phys.*, vol. 95, no. 7, pp. 3778–3784, 2004.

[28] L. Jylhä, S. Maslovski, and S. Tretyakov, "Higher order resonant modes of a metasolenoid," *J. Electromagnetic Waves and Applications*, vol. 19, no. 10, pp. 1327–1342, 2005.

[29] A. Tonning, "Energy density in continuous electromagnetic media," *IRE Trans. Antennas Propag.*, vol. 8, no. 4, pp. 428–434, 1960.

[30] J. Askne and B. Lind, "Energy of electromagnetic waves in the presence of absorption and dispersion," *Phys. Rev. A*, vol. 2, no. 6, pp. 2335–2340, 1970.

[31] R. Loudon, "The propagation of electromagnetic energy through an absorbing dielectric," *J. Phys. A: Gen. Phys.*, vol. 3, pp. 233–245, 1970.

[32] R. Ruppin, "Electromagnetic energy density in a dispersive and absorptive material," *Phys. Lett. A*, vol. 299, pp. 309–312, 2002.

[33] H. Cao and T. J. Cui, "Electromagnetic energy in absorbtive and dispersive medium based on the assembly of atomic oscillations," *Microwave Opt. Technol. Lett.*, vol. 48, no. 11, pp. 2288–2291, 2006.

[34] A. D. Yaghjian, "Improved formulas for the Q of antennas with highly lossy dispersive materials," *IEEE Antennas Wireless Propag. Lett.*, vol. 5, pp. 365–369, 2006.

[35] W. Webb, *The future of wireless communications*. Boston: Artech House, 2001.

[36] K. Hirasawa and M. Haneishi, Eds., *Analysis, design, and measurements of small and low-profile antennas*. London: Artech House, 1992.

[37] D. M. Pozar and D. H. Schaubert, Eds., *Microstrip antennas: The analysis and design of microstrip antennas and arrays*. Piscataway, NJ: IEEE Press, 1995.

[38] J. Ollikainen, *Design and implementation techniques of wideband mobile communications antennas*. Helsinki University of Technology: PhD Dissertation, 2004.

[39] I. J. Bahl and P. Bhartia, *Microstrip antennas*. Massachusettes: Artech House, 1980.

[40] K. R. Carver and J. W. Mink, "Microstrip antenna technology," *IEEE Trans. Antennas Propag.*, vol. AP–29, no. 1, pp. 2–24, 1981.

[41] D. M. Pozar, "Microstrip antennas," *Proc. IEEE.*, vol. 80, pp. 79–91, 1992.

[42] C. A. Balanis, *Antenna theory: Analysis and design*. New York: John Wiley & Sons, 1997.

[43] R. K. Mongia, A. Ittipiboon, and M. Cuhaci, "Low profile dielectric resonator antennas using a very high permittivity material," *Electron Lett.*, vol. 30, no. 17, pp. 1362–1363, 1994.

[44] Y. Hwang, Y. P. Zhang, G. X. Zheng, and T. K. C. Lo, "Planar inverted F antenna loaded with high permittivity material," *Electron Lett.*, vol. 31, no. 20, pp. 1710–1712, 1995.

[45] J. S. Colburn and Y. Rahmat-Samii, "Patch antennas on externally perforated high dielectric constant substrates," *IEEE Trans. Antennas Propag.*, vol. 47, no. 12, pp. 1785–1794, 1999.

[46] D. R. Jackson and N. G. Alexopoulos, "Simple approximate formulas for input resistance, bandwidth, and efficiency of a resonant rectangular patch," *IEEE Trans. Antennas Propag.*, vol. 39, no. 3, pp. 407–409, 1991.

[47] R. C. Hansen and M. Burke, "Antennas with magneto-dielectrics," *Microwave Opt. Technol. Lett.*, vol. 26, no. 2, pp. 75–78, 2000.

[48] O. Edvardsson, "On the influence of capacitive and inductive loading on different types of small patch / PIFA structures for use on mobile phones," in *Proc. ICAP Int. Conf. Antennas Propag.*, Manchester, UK, Apr. 17–20, 2001, pp. 17–20.

[49] A. N. Lagarkov, A. V. Osipov, K. N. Rozanov, and S. N. Starostenko, "Microwave composites filled with thin ferromagnetic films. Part I. Theory," in *Proc. Symposium R, Electromagnetic Materials*, Singapore, July 3–8, 2005, pp. 74–77.

[50] K. N. Rozanov, Private communication, 2006.

[51] G. Perrin, O. Acher, J. C. Peuzin, and N. Vukadinovic, "Sum rules for gyromagnetic permeability of ferromagnetic thin films: Theoretical and experimental results," *J. Magnetism and Magnetic Materials*, vol. 157–158, pp. 289–290, 1996.

[52] O. Acher and A. L. Adenot, "Bounds on the dynamic properties of magnetic materials," *Phys. Rev. B*, vol. 62, no. 17, pp. 11 324–11 327, 2000.

[53] P. M. T. Ikonen, P. Alitalo, and S. A. Tretyakov, "On impedance bandwidth of resonant patch antennas implemented using structures with engineered dispersion," arxiv: physics/0611101, Nov. 2006.

[54] S. A. Tretyakov, S. I. Maslovski, A. A. Sochava, and C. R. Simovski, "The influence of complex material coverings on the quality factor of simple radiating systems," *IEEE Trans. Antennas Propag.*, vol. 53, no. 3, pp. 965–970, 2005.

[55] P. Ikonen, S. Maslovski, and S. Tretyakov, "PIFA loaded with artificial magnetic material: Practical example for two utilization strategies," *Microwave Opt. Technol. Lett.*, vol. 46, no. 3, pp. 205–210, 2005.

[56] K. N. Rozanov, "Ultimate thickness to bandwidth ratio of radar absorbers," *IEEE Trans. Antennas Propag.*, vol. 48, no. 8, pp. 1230–1234, 2000.

[57] H. Mosallaei and K. Sarabandi, "Magneto-dielectrics in electromagnetics: Concept and applications," *IEEE Trans. Antennas Propag.*, vol. 52, no. 6, pp. 1558–1567, 2004.

[58] S. Yoon and R. W. Ziolkowski, "Bandwidth of a microstrip patch antenna on a magneto-dielectric substrate," in *Proc. IEEE Antennas Propag. Soc. Int. Symposium*, Columbus, Ohio, Jun. 22–27, 2003, pp. 297–300.

[59] H. Mosallaei and K. Sarabandi, "Engineered meta-substrates for antenna miniaturization," in *Proc. 2004 URSI Int. Symposium on Electromagn. Theory*, Pisa, Italy, May 23–27, 2004, pp. 191–193.

[60] M. K. Kärkkäinen, S. A. Tretyakov, and P. Ikonen, "Numerical study of a PIFA with dispersive material fillings," *Microwave Opt. Technol. Lett.*, vol. 45, no. 1, pp. 5–8, 2005.

[61] M. E. Ermutlu, C. R. Simovski, M. K. Kärkkäinen, P. Ikonen, S. A. Tretyakov, and A. A. Sochava, "Miniaturization of patch antennas with new artificial magnetic layers," in *Proc. 2005 IEEE Int. Workshop on Antenna Technology*, Singapore, Mar. 7–9, 2005, pp. 87–90.

[62] M. E. Ermutlu, C. R. Simovski, M. K. Kärkkäinen, P. Ikonen, A. A. Sochava, and S. A. Tretyakov, "Patch antennas with new artificial magnetic layers," arxiv: physics/0504075, Apr. 2005.

[63] M. K. Kärkkäinen and P. Ikonen, "Patch antenna with stacked split-ring resonators as artificial magneto-dielectric substrate," *Microwave Opt. Technol. Lett.*, vol. 46, no. 6, pp. 554–556, 2005.

[64] K. Buell, H. Mosallaei, and K. Sarabandi, "A substrate for small patch antennas providing tunable miniaturization factors," *IEEE Trans. Microw. Theory Tech.*, vol. 54, no. 1, pp. 135–145, 2006.

[65] H. Mosallaei and K. Sarabandi, "Design and modeling of patch antenna printed on magneto-dielectric embedded-circuit metasubstrate," *IEEE Trans. Antennas Propag.*, vol. 55, no. 1, pp. 45–52, 2007.

[66] P. M. T. Ikonen and S. A. Tretyakov, "Comments on "Design and modeling of patch antenna printed on magneto-dielectric embedded-circuit metasubstrate"," unpublished (submitted to *IEEE Trans. Antennas Propag.*, Jan. 2007).

[67] R. K. Mishra, S. S. Pattnaik, and N. Das, "Tuning of microstrip antenna on ferrite substrate," *IEEE Trans. Antennas Propag.*, vol. 41, no. 2, pp. 230–233, 1993.

[68] A. R. Mishra, *Fundamentals of cellular network planning and optimization.* New York: John Wiley & Sons, 2004.

[69] R. E. Collin, *Field theory of guided waves*, 2nd ed. Piscataway, NJ: IEEE Press, 1991.

[70] C. A. Moses and N. Engheta, "Electromagnetic wave propagation in the wire medium: A complex medium with long thin inclusions," *Wave Motion*, vol. 34, pp. 301–307, 2001.

[71] J. B. Brown, "Artificial dielectrics," in *Progress in Dielectrics*, 2nd ed., J. B. Birks and J. H. Schulman, Eds. London: Heywood Co. Ltd., 1960, pp. 193–225.

[72] W. Rotman, "Plasma simulation by artificial dielectrics and parallel plate media," *IRE Trans. Antennas Propag.*, vol. 10, pp. 82–95, 1962.

[73] P. Belov, S. A. Tretyakov, and A. J. Viitanen, "Dispersion and reflection properties of artificial media formed by regular lattices of ideally conducting wires," *J. Electromagnetic Waves and Applications*, vol. 16, no. 8, pp. 1153–1170, 2002.

[74] S. I. Maslovski, S. A. Tretyakov, and P. A. Belov, "Wire media with negative effective permittivity: A quasi static model," *Microwave Opt. Technol. Lett.*, vol. 35, no. 1, pp. 47–51, 2002.

[75] P. A. Belov, C. R. Simovski, and S. A. Tretyakov, "Two-dimensional electromagnetic crystals formed by reactively loaded wires," *Phys. Rev. E*, vol. 66, p. 036610, 2002.

[76] J.-M. Lourtioz, A. de Lustrac, F. Gadot, S. Rowson, A. Chelnokov, T. Brillat, A. Ammouche, J. Danglot, O. Vanbésien, and D. Lippens, "Toward controllable photonic crystals for centimeter- and millimeter-wave devices," *J. Lightw. Technol.*, vol. 17, no. 11, pp. 2025–2031, 1999.

[77] V. Kuzmiak, A. A. Maradudin, and F. Pincemin, "Photonic band structures of two-dimensional systems containing metallic components," *Phys. Rev. B*, vol. 50, no. 23, pp. 16 835–16 844, 1994.

[78] N. A. Nicorovici, R. C. McPhedran, and L. C. Botten, "Photonic band gaps for arrays of perfectly conducting cylinders," *Phys. Rev. E*, vol. 52, no. 1, pp. 1135–1145, 1995.

[79] M. M. Sigalas, C. T. Chan, K.-M. Ho, and C. M. Soukoulis, "Metallic photonic band-gap materials," *Phys. Rev. B*, vol. 52, no. 16, pp. 11 744–11 751, 1995.

[80] P. A. Belov, R. Marqués, S. I. Maslovski, I. S. Nefedov, M. Silverinha, C. R. Simovski, and S. A. Tretyakov, "Strong spatial dispersion in wire media in the very large wavelength limit," *Phys. Rev. B*, vol. 67, p. 113103, 2003.

[81] C. R. Simovski and P. A. Belov, "Low frequency spatial dispersion in wire media," *Phys. Rev. E*, vol. 70, p. 046616, 2004.

[82] R. C. Hansen, "Current induced on a wire: Implications for connected arrays," *IEEE Antennas Wireless Propag. Lett.*, vol. 2, pp. 288–289, 2003.

[83] P. Ikonen, *Artificial wire medium with antenna applications.* Helsinki University of Tecnology: Master's Thesis, 2005.

[84] C. R. Simovski and S. He, "Antennas based on modified metallic photonic bandgap structures consisting of capacitively loaded wires," *Microwave Opt. Technol. Lett.*, vol. 31, no. 5, pp. 214–221, 2001.

[85] W. E. Kock, "Metal-lens antennas," *Proc. IRE*, vol. 34, pp. 828–836, 1946.

[86] ——, "Metallic delay lenses," *Bell System Technical J.*, vol. 27, pp. 58–82, 1948.

[87] K. E. Golden, "Plasma simulation with an artificial dielectric in a horn geometry," *IEEE Trans. Antennas Propag.*, vol. 13, no. 4, pp. 587–594, 1965.

[88] I. J. Bahl and K. C. Gupta, "A leaky-wave antenna using an artificial dielectric medium," *IEEE Trans. Antennas Propag.*, vol. 22, no. 1, pp. 119–122, 1974.

[89] ——, "Frequency scanning leaky-wave antennas using artificial dielectrics," *IEEE Trans. Antennas Propag.*, vol. 23, no. 4, pp. 584–589, 1975.

[90] G. Poilasne, J. Lenormand, P. Pouliguen, K. Mahdjoubi, C. Terret, and P. Gelin, "Theoretical study of interactions between antennas and metallic photonic bandgap materials," *Microwave Opt. Technol. Lett.*, vol. 15, no. 6, pp. 384–389, 1997.

[91] G. Poilasne, P. Pouliguen, K. Mahdjoubi, J. Lenormand, C. Terret, and P. Gelin, "Theoretical study of grating lobes reduction using metallic photonic bandgap materials (MPBG)," *Microwave Opt. Technol. Lett.*, vol. 18, no. 1, pp. 32–41, 1998.

[92] G. Poilasne, P. Pouliguen, K. Mahdjoubi, C. Terret, P. Gelin, and L. Desclos, "Influence of metallic photonic band-gap (MPBG) materials interface on dipole radiation characteristics," *Microwave Opt. Technol. Lett.*, vol. 18, no. 6, pp. 407–410, 1998.

[93] ——, "Experimental radiation pattern of dipole inside metallic photonic band-gap material," *Microwave Opt. Technol. Lett.*, vol. 22, no. 1, pp. 10–16, 1999.

[94] G. Poilasne, P. Pouliguen, K. Mahdjoubi, L. Desclos, and C. Terret, "Active metallic photonic band-gap materials (MPBG): Experimental results on beam shaper," *IEEE Trans. Antennas Propag.*, vol. 48, no. 1, pp. 117–119, 2000.

[95] H. Boutayeb, T. A. Denidni, A. R. Sebak, and L. Talbi, "Design of elliptical electromagnetic bandgap structures for directive antennas," *IEEE Antennas Wireless Propag. Lett*, vol. 4, pp. 93–96, 2005.

[96] S. He, C. R. Simovski, and M. Popov, "An explicit and efficient method for obtaining the radiation characteristics of wire antennas in metallic photonic bandgap structures," *Microwave Opt. Technol. Lett.*, vol. 26, no. 2, pp. 67–73, 2000.

[97] S. He, M. Popov, M. Qiu, Z. Liao, and C. Simovski, "Explicit formulas for obtaining the radiation characteristics of an antenna based on a three dimensional metallic photonic bandgap structures," *Microwave Opt. Technol. Lett.*, vol. 29, no. 6, pp. 376–381, 2001.

[98] A. de Lustrac, F. Gadot, E. Akmansoy, and T. Brillat, "High-directivity planar antenna using controllable photonic bandgap material at microwave frequencies," *Appl. Phys. Lett.*, vol. 78, no. 26, pp. 4196–4198, 2001.

[99] R. Milne, "Dipole array lens antenna," *IEEE Trans. Antennas Propag.*, vol. 30, no. 4, pp. 704–712, 1982.

[100] P. Ratajczak, P. Brachat, and J. M. Fargeas, "An adaptive beam steering antenna for mobile communications," in *Proc. IEEE Antennas Propag. Soc. Int. Symposium*, Albuquerque, USA, Jul. 9–14, 2006, pp. 418–421.

[101] (Last cited: February 19, 2007) The www–page of the Kathrein group. [Online]. Available: http://www.kathrein.com/

[102] B. Gralak, S. Enoch, and G. Tayeb, "Anomalous refractive properties of photonic crystals," *J. Opt. Soc. Am. A*, vol. 17, no. 6, pp. 1012–1020, 2000.

[103] G. Guida, D. Maystre, G. Tayeb, and P. Vincent, "Mean-field theory of two-dimensional metallic photonic crystals," *J. Opt. Soc. Am. B*, vol. 15, no. 8, pp. 2308–2315, 1998.

[104] B. T. Schwartz and R. Piestun, "Total external reflection from metamaterials with ultralow refractive index," *J. Opt. Soc. Am. B*, vol. 20, no. 12, pp. 2448–2453, 2003.

[105] S. Enoch, G. Tayeb, P. Sabouroux, N. Guérin, and P. Vincent, "A metamaterial for directive emission," *Phys. Rev. Lett.*, vol. 89, no. 21, p. 213902, 2002.

[106] S. Enoch, G. Tayéb, and B. Gralak, "The richness of the dispersion relation of electromagnetic bandgap materials," *IEEE Trans. Antennas Propag.*, vol. 51, no. 10, pp. 2659–2666, 2003.

[107] G. Lovat, P. Burghignoli, F. Capolino, D. R. Jackson, and D. R. Wilton, "Analysis of directive radiation from a line source in a metamaterial slab with low permittivity," *IEEE Trans. Antennas Propag.*, vol. 54, no. 3, pp. 1017–1030, 2006.

[108] H. Boutayeb and T. A. Denidni, "Analysis and design of a high-gain antenna based on metallic crystals," *J. Electromagnetic Waves and Applications*, vol. 20, no. 5, pp. 599–614, 2006.

[109] G. Tayeb and D. Maystre, "Rigorous theoretical study of finite-size two-dimensional photonic crystals doped by microcavities," *J. Opt. Soc. Am. A*, vol. 14, no. 12, pp. 3323–3332, 1997.

[110] M. Thévenot, C. Cheype, A. Reineix, and B. Jecko, "Directive photonic-bandgap antennas," *IEEE Trans. Microw. Theory Tech.*, vol. 47, no. 11, pp. 2115–2122, 1999.

[111] C. Cheype, C. Serier, M. Thévenot, T. Monédiére, A. Reineix, and B. Jecko, "An electromagnetic bandgap resonator antenna," *IEEE Trans. Antennas Propag.*, vol. 50, no. 9, pp. 1285–1290, 2002.

[112] B. Temelkuran, M. Bayindir, E. Ozbay, R. Biswas, M. M. Sigalas, G. Tuttle, and K.-M. Ho, "Photonic crystal-based resonant antenna with a very high directivity," *J. Appl. Phys.*, vol. 87, no. 1, pp. 603–605, 2000.

[113] F. Ghanem, G. Y. Delisle, T. A. Denidni, and K. Ghanem, "A directive dual-band antenna based on metallic electromagnetic crystals," *IEEE Antennas Wireless Propag. Lett.*, vol. 5, pp. 384–387, 2006.

[114] A. H. Sihvola, "Electromagnetic emergence in metamaterials: Deconstraction of terminology of comlex media," in *Advances in Electromagnetics of Complex Media and Metamaterials*, S. Zouhdi, A. H. Sihvola, and M. Arslane, Eds. Dordrecht, the Netherlands: Kluver Academic Publishers, 2003, pp. 1–18.

[115] (Last cited: February 19, 2007) Metamaterials home-page, future projects of the Defence Advanced Research Projects Agency (DARPA). [Online]. Available: http://www.darpa.mil/dso/thrust/matdev/metamat.htm

[116] (Last cited: February 19, 2007) The www–page of the European Network of Excellence Metamorphose. [Online]. Available: http://www.metamorphose-eu.org/

[117] D. R. Smith, W. J. Padilla, D. C. Vier, S. C. Nemat-Nasser, and S. Schultz, "Composite medium with simultaneously negative permeability and permittivity," *Phys. Rev. Lett.*, vol. 84, no. 18, pp. 4184–4187, 2000.

[118] R. A. Shelby, D. R. Smith, and S. Schultz, "Experimental verification of a negative index of refraction," *Science*, vol. 5514, no. 292, pp. 77–79, 2001.

[119] T. Weiland, R. Schuhmann, R. B. Greegor, C. G. Parazzoli, A. M. Vetter, D. R. Smith, D. C. Vier, and S. Schultz, "*Ab initio* numerical simulation of left-handed metamaterials: Comparison of calculations and experiments," *J. Appl. Phys.*, vol. 90, no. 10, pp. 5419–5424, 2001.

[120] P. Markos and C. M. Soukoulis, "Numerical studies of left-handed materials and arrays of split ring resonators," *Phys. Rev. E*, vol. 65, no. 3, p. 036622, 2002.

[121] C. R. Simovski, P. A. Belov, and S. He, "Backward wave region and negative material parameters of a structure formed by lattices of wires and split-ring resonators," *IEEE Trans. Antennas Propag.*, vol. 51, no. 10, pp. 2582–2591, 2003.

[122] N. Engheta, M. Silveirinha, A. Alu, and A. Salandrino, "Scattering and reflection properties of low-epsilon metamaterials shells and bends," in *Proc. of joint ICEAA'05 and EESC'05 Conf.*, Torino, Italy, Sept. 12–16, 2005, pp. 101–104.

[123] M. Silveirinha and N. Engheta, "Tunneling of electromagnetic energy through subwavelength channels and bends using ϵ-near-zero materials," *Phys. Rev. Lett.*, vol. 97, p. 157403, 2006.

[124] R. A. Shelby, D. R. Smith, S. C. Nemat-Nasser, and S. Schultz, "Microwave transmission through two-dimensional, isotropic, left-handed metamaterial," *Appl. Phys. Lett.*, vol. 78, no. 4, pp. 489–491, 2001.

[125] R. W. Ziolkowski and E. Heyman, "Wave propagation in media having negative permittivity and permeability," *Phys. Rev. E*, vol. 64, p. 056625, 2001.

[126] J. Pacheo, T. M. Grzegorczyk, B.-I. Wu, Y. Zhang, and J. A. Kong, "Power propagation in homogeneous isotropic frequency-dispersive left-handed media," *Phys. Rev. Lett.*, vol. 89, no. 25, pp. 257 401–4, 2002.

[127] R. W. Ziolkowski, "Propagation in and scattering from a matched metamaterial having a zero index of refraction," *Phys. Rev. E*, vol. 70, p. 046608, 2004.

[128] P. F. Loschialpo, D. W. Forester, D. L. Smith, and F. J. Rachford, "Optical properties of an ideal homogeneous causal left-handed material slab," *Phys. Rev. E*, vol. 70, p. 036605, 2004.

[129] C. Monzon, P. Loschialpo, and D. W. Forester, "Zero-permeability materials: An artifact of losses in left-handed media," *IEE Proc. Microwaves, Antennas Propag.*, vol. 152, no. 6, pp. 465–470, 2005.

[130] L. B. Felsen and N. Marcuvitz, *Radiation and scattering of waves.* Piscataway, NJ: IEEE Press, 1991.

[131] I. V. Lindell and E. Alanen, "Exact image theory for the Sommerfeld haf-space problem, part III: General formulation," *IEEE Trans. Antennas Propag.*, vol. 32, no. 10, pp. 1027–1030, 1984.

[132] M. I. Oksanen, S. A. Tretyakov, and I. V. Lindell, "Vector circuit theory for isotropic and chiral slabs," *J. Electromagnetic Waves and Applications*, vol. 4, no. 7, pp. 613–643, 1990.

[133] M. I. Oksanen, P. K. Koivisto, and S. A. Tretyakov, "Vector circuit method applied for chiral slab waveguides," *J. Lightw. Technol.*, vol. 10, no. 2, pp. 150–155, 1992.

[134] A. J. Viitanen and P. P. Puska, "Reflection of obliquely incident plane wave from chiral slab backed by soft and hard surface," *IEE Proc. Microw. Antennas Propag.*, vol. 146, no. 4, pp. 271–276, 1999.

[135] M. I. Oksanen, J. Hänninen, and S. A. Tretyakov, "Vector circuit method for calculating reflection and transmission of electromagnetic waves in multilayer chiral structures," *IEE Proc. pt. H – Microwaves, Antennas Propag.*, vol. 138, no. 6, pp. 513–520, 1991.

[136] J. B. Pendry, "Negative refraction makes a perfect lens," *Phys. Rev. Lett.*, vol. 85, no. 18, pp. 3966–3969, 2000.

[137] (Last cited: February 19, 2007) The www–page of Prof. D. R. Smith, Duke University. [Online]. Available: http://www.ee.duke.edu/∼drsmith/

[138] M. Notomi, "Theory of light propagation in strongly modulated photonic crystals: Refractionlike behavior in the vicinity of the photonic band gap," *Phys. Rev. B*, vol. 62, no. 16, pp. 10 696–10 705, 2000.

[139] P. V. Parimi, W. T. Lu, P. Vodo, and S. Sridhar, "Imaging by flat lens using negative refraction," *Nature*, vol. 426, p. 404, 2003.

[140] C. Luo, S. G. Johnson, J. D. Joannopoulos, and J. B. Pendry, "All-angle negative refraction without negative effective index," *Phys. Rev. B*, vol. 65, p. 201104, 2002.

[141] C. Luo, S. G. Johnson, J. D. Joannopoulos, and J. Pendry, "Subwavelength imaging in photonic crystals," *Phys. Rev. B*, vol. 68, p. 045115, 2003.

[142] Z.-Y. Li and L.-L. Lin, "Evaluation of lensing in photonic crystal slabs exhibiting negative refraction," *Phys. Rev. B*, vol. 68, p. 245110, 2003.

[143] H.-T. Chien, H.-T. Tang, C.-H. Kuo, C.-C. Chen, and Z. Ye, "Directed diffraction without negative refraction," *Phys. Rev. B*, vol. 70, p. 113101, 2004.

[144] C.-H. Kuo and Z. Ye, "Optical transmission of photonic crystal structures formed by dielectric cylinders: Evidence for non-negative refraction," *Phys. Rev. E*, vol. 70, p. 056608, 2004.

[145] X. Zhang, "Absolute negative refraction and imaging of unpolarized electromagnetic waves by two dimensional photonic crystals," *Phys. Rev. B*, vol. 70, p. 205102, 2004.

[146] D. N. Chigrin, S. Enoch, C. M. S. Torres, and G. Tayeb, "Self-guiding in two-dimentional photonic crystals," *Optics Express*, vol. 11, no. 10, pp. 1203–1211, 2003.

[147] S. A. Tretyakov, Private communication, 2005.

[148] P. A. Belov, Y. Hao, and S. Sudhakaran, "Subwavelength microwave imaging using an array of parallel conducting wires as a lens," *Phys. Rev. B*, vol. 73, p. 033108, 2006.

[149] F. Mesa, M. J. Freire, R. Marques, and J. D. Baena, "Three dimensional superresolution in metamaterial slab lenses: Experiment and theory," *Phys. Rev. B*, vol. 72, p. 235117, 2005.